Progress in Organic Coatings 192 (2024) 108469

Contents lists available at ScienceDirect

Progress in Organic Coatings

journal homepage: www.elsevier.com/locate/porgcoat

Review

Recent progress in understanding filiform corrosion on organic coated steel: A comprehensive review

Andrea Cristoforetti *, Stefano Rossi, Flavio Deflorian, Michele Fedel

Department of Industrial Engineering, University of Trento, via Sommarive n. 9, 38123 Trento, Italy

ARTICLE INFO

Keywords:
Organic coatings
Filiform corrosion
Steel
Coatings delamination
Failure mechanism
corrosion protection

ABSTRACT

Organic coatings delamination and corrosion pose an ongoing challenge in materials science. This review explores the knowledge of corrosion mechanisms in painted steel structures up to date, focusing on filiform corrosion (FFC) investigating its mechanisms, and discussing available prevention strategies alongside their suitability. First reported in the 1940s, FFC garnered significant attention in the subsequent decades, particularly in the study of coated aluminum, and very recently magnesium alloys. However, its consideration as a component of steel degradation remained comparatively limited during this period. Despite advancements, comprehensive analysis of FFC has been infrequent, prompting a call for an updated critical analysis. This survey emphasizes the necessity for organized FFC mitigation strategies, discussing alternatives and emerging trends. It underscores FFC's potential role as a precursor to general corrosion, emphasizing the economic implications of aesthetic damage. This review aims to fill gaps, assess current knowledge, and pave the way for future research in the realm of organic-coated steel corrosion.

1. Introduction

The degradation of painted steel structures frequently involves various forms of corrosion, with numerous aging mechanisms at play. Each service environment may give rise to distinct failure modes. Cathodic delamination is believed to represent the predominant corrosion morphology, resulting in coating delamination and diffuse substrate rusting. However, a lesser-known form of corrosion, termed filiform corrosion (FFC), characterized by anodic undermining, also occurs on painted steel.

Sharman (1944) conducted the initial investigation on FFC [1], depicting it as a deterioration process that leads to the development of filamentous corrosion products beneath protective coatings. FFC typically occurs in moist environments, originating from surface imperfections in the protective film in the presence of soluble ionic species. This type of corrosion commonly affects steel, aluminum [2–10], and magnesium [11–13] surfaces coated with organic films such as lacquer or paint. The FFC occurrence varies depending on the specific metal substrate, indicating the existence of distinct underlying mechanisms. The participation of ions with different valences and their inclination to create compounds with varied chemical and physical characteristics lead to peculiar observable morphologies. The filaments associated with FFC exhibit a slender and shallow profile, yet they can attain significant lengths (in the order of several centimeters). The width and thickness of these filaments appear to be influenced by the properties of the organic coating, such as the adhesion to the substrate and the specific type of salt that initiates corrosion. Filaments typically display a branching structure and exhibit directional growth. In metals with a distinctive processing direction, corrosion threads tend to develop along that specific orientation. Alternatively, in the absence of a characteristic extrusion direction, filament growth occurs in random directions, originating from defects in the coating or weak interfacial spots. The visual representation of corrosion filament in the case of an acrylic-coated steel substrate is depicted in Fig. 1. A distinct separation between two different areas is discernible along the filament. This unique distribution of corrosion products has been noted to form a "V-shaped" head, characterized by a clearly defined boundary between the designated "head" (the leading portion) and "tail" (the rear part). The color contrast in the two regions is attributed to the presence of different iron ions-based compounds, emphasizing the distinct chemical composition of the head and tail regions, and therefore the diverse reactions involved.

Although the first observation of FFC on painted steel dates back to

* Corresponding author.
E-mail addresses: andrea.cristoforetti@unitn.it (A. Cristoforetti), stefano.rossi@unitn.it (S. Rossi), flavio.deflorian@unitn.it (F. Deflorian), michele.fedel@unitn.it (M. Fedel).

https://doi.org/10.1016/j.porgcoat.2024.108469
Received 5 March 2024; Received in revised form 8 April 2024; Accepted 19 April 2024
Available online 27 April 2024

the 1940s, the subsequent decades have witnessed a growing interest in this phenomenon, particularly in the context of aluminum and magnesium. This heightened attention is primarily driven by the significance of the issue in the aeronautic and automotive industries, where the use of lighter alloys is prevalent. Despite this increased focus, there has been a notable scarcity of investigations specifically centered on steel substrates. In the subsequent years, notable contributions were made to understanding FFC. Ruggeri and Beck (1983) [14] were among the pioneers, and later, in 1996, Bautista [15] provided a comprehensive review encompassing the state of the art knowledge related to this failure mechanism. While the latest review of advancements in this field by McMurray and Williams within Volume 2 of Shreir's Corrosion dates back to 2010 [16]. Their reviews covered causes, and mitigation strategies and highlighted certain unresolved issues, along with suggestions for future research. However, it has been >25 years since the last comprehensive survey, and during this time, several research groups have made significant strides in enhancing our understanding of FFC in organic-coated steel.

FFC occurrences in defective coated steel have been established to comprise two phases: (i) contaminants-driven initiation and (ii) linear front propagation [17,18]. In recent years, utilizing various electrochemical techniques such as scanning Kelvin probe (SKP) [19–22], electrochemical impedance spectroscopy (EIS) [23] scanning vibrating electrode techniques (SVET) [24,25], and micropotentiometry (SECM) [24], substantial evidence has been gathered to discern anodic and cathodic activities, marked by pronounced spatial separation. Furthermore, recent literature has provided new insights into the corrosive environment developing at the metal-paint interface. It also explores the influence of environmental factors, such as oxygen, contaminants, and humidity, on FFC morphology, growth rate, and initiation triggers [18,26–28]. The average growth rate of filiform corrosion in coated steel typically falls within the range of 0.2 to 0.9 mm per day (see Table 1). Significantly, the growth rate of threads in steel is approximately one order of magnitude higher than that observed in aluminum [15,29]. Corrosion damage tends to escalate with higher environmental salinity [28]. Interestingly, the thickness of the protective film does not exhibit a definitive influence on the rate at which the filiform corrosion process develops [14].

Given these advancements and the evolving landscape of research in this domain, there is a recognized need for an updated, comprehensive, and critical analysis of the achievements to date. Such an analysis would provide valuable insights into the current state of knowledge, identify gaps, and set the stage for future investigations in the field. Furthermore, there is a need for organization in the field of FFC mitigation, encompassing a discussion on the currently available alternatives and emerging trends in research for protecting against this failure mechanism. While FFC is commonly perceived as causing aesthetic damage to the coating system [30], it can potentially serve as an initiation event for the general corrosion of the steel substrate [18] along with paint delamination. Although the expansion of filaments at the metal-paint interface does not harm the mechanical integrity of the structure, as the metal substrate dissolution depth is approximately 10 μm [14], the situation changes when coating delamination occurs. With coating detachment and the subsequent deposition of iron rust with a thickness of tens of μm, the protective properties of the paints wear off. This allows both humidity and oxygen to freely reach the exposed substrate, resulting in more severe general corrosion. At this juncture, the significance of preventing and mitigating FFC becomes evident to halt further damage progression. Moreover, the undesirable alteration of the appearance of painted goods over time is no longer acceptable, as any potential noncompliance reflects on maintenance costs and the frequency of scheduled service events.

In addressing this issue, various efforts have been dedicated to adapting existing prevention and protection techniques, including conversion coatings (CCs) and inhibitors to counteract FFC. Additionally, novel materials have recently been introduced to mitigate this phenomenon. Notably, several stimuli-responsive micro/nanocontainers for the controlled release of corrosion inhibitors are gaining increasing attention in this field. Some promising results from these endeavours focusing on steel substrates have been published encouragingly [31,32]. Further efforts are necessary for the prevention of FFC, and this study aims to establish guidelines for the design of protective methods. The objective is to adapt these methods in alignment with the accepted corrosion mechanisms.

In this review, we present a comprehensive overview of experimental research conducted to date in the realm of filiform corrosion occurring on painted steel substrates. Emphasis is placed on elucidating the mechanisms underlying delamination from an electrochemical perspective, examining various models proposed over the years and their correlation with factors that precipitate this corrosion phenomenon. This manuscript encompasses a thorough compilation of laboratory studies simulating weathering conditions and outdoor exposure scenarios where FFC occurs, discussing associated features such as propagation rates and encountered atmospheric parameters. Additionally, we discuss the main mitigation strategies explored over the years, ranging from the integration of inhibitors and pigments within the paint formulation to the application of surface treatments, aiming to quantitatively compare their efficacy in inhibiting corrosion.

2. The phenomenon: Causes and outcomes

FFC in organic coated steel constitutes a localized corrosive

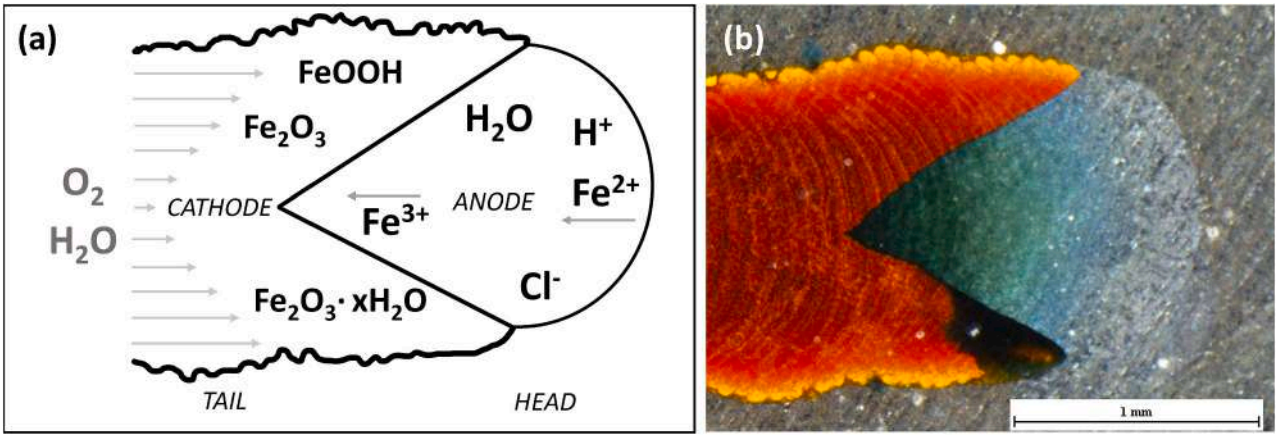

Fig. 1. A schematic representation of the filiform corrosion (FFC) mechanism is illustrated in (a), accompanied by an example of filament appearance captured through optical imaging via the Acrylic clearcoat in (b). Adapted with permission from Ref. [24].

Table 1
Propagation rate on organic coated steel sample aged after the introduction of an artificial scratch.

Coating	Thickness (μm)	Initiating electrolyte	Relative humidity (%)	T (°C)	Propagation rate *(mm/day) **(mm^2/day)	References
Lacquer	–	CH_3COOH	–	–	0.85*	Sharman 1944 [1]
Varnish	–	CH_3COOH	86	24	0.5*	Van Loo 1953 [28]
Urea-alkyd	–	–	85	Room	0.25*	Slabaugh and Grotheer 1954 [34]
Varnish	–	–	60	Room	0.28*	Preston and Sanyal 1956 [35]
Polyurethane	25–50	NaCl	90	23	0.16–0.5*	Ruggeri and Beck 1983 [14]
PVB	20	NaCl	93	20	0.46 *	Williams et al. 2003 [17]
polyurethane	100	HCl	85	40	0.83*	Catubig et at. 2011 [36]
PVB	30	$FeCl_2$	93	20	0.55*	Watson et al. 2014 [27]
PVB	10	$FeCl_2$	95	25	0.12**	Glover et al. 2017 [37]
Acrylic	75	NaCl	80	40	0.27*	Cristoforetti et al. 2023 [26]

phenomenon characterized by linear patterns of progression. Its morphological features include the presence of distinct anodic and cathodic reaction sites at the filament tip. The progression of FFC involves the linear advancement of the thread's head along a path, with the resultant corrosion products forming a developing tail. Optimal conditions for FFC initiation require a relative humidity (r.h.%) within the 60–95 % range [15,18,33], coupled with the presence of contaminant-aggressive ions, typically chlorides and sulphates, in the atmosphere [14,17,38]. Elevated r.h.% values disrupt linear filament propagation, favouring a failure mechanism that induces blistering (Fig. 2) [18,35,39–41]. This phenomenon has been specifically emphasized in cyclic cabinet tests, exemplified by ASTM G85 – Annex 5 [42]. In these tests designed to emulate natural exposure conditions, the humidity varies from 40 % to the point of saturated saline fog. Notably, these controlled experiments reveal a simultaneous manifestation of both FFC and blistering under these elevated humidity conditions [18]. A hypothesis made on this phenomenon states that at elevated relative humidity levels, the increased water content within the polymer accelerates the rate of oxygen diffusion through the coating. Thus, this heightened oxygen permeability facilitates the oxygen reduction reaction encompassing the location of iron dissolution. Consequently, under these conditions, the unidirectional nature of the filament is compromised, and there is a preference for the formation of blisters [18,19,28,43]. Nevertheless, there is currently no experimental validation for this plausible interpretation. Additionally, an explanation for the emergence of this humidity threshold, varying between 93 % and 100 % depending on the specific coating system under consideration, is absent from the available information [18].

On steel substrates FFC exemplifies an oxygen concentration cell beneath the paint, where the distinct color and shade gradient enables easy differentiation between the leading head and the developing tail (Fig. 1) [24,26,27]. Various factors influence the susceptibility of painted structures to filiform corrosion (FFC). The key parameters include (i) humidity levels and (ii) oxygen availability, the presence of contaminant species (iii) necessary for FFC initiation, the impact of temperature (iv) on coating properties and chemical kinetics, the quality of metal-paint adhesion (v) related to surface preparation, pretreatments/conversion layers (vi), and paint chemistry (vii), as well as the existence of weaknesses and defective spots in the coating layer (viii). The conditions conducive to FFC appear to be more prevalent than the extremely high humidity levels associated with cathodic delamination [18,28,41]. This underscores the significance of conducting in-depth investigations into the mechanisms leading to paint failure in the context of FFC. The main conditions available in the literature are summarized in Table 2.

Going through the environmental parameters, humidity emerges as a crucial factor in triggering FFC, setting it apart from cathodic delamination. Moreover, the necessary concentration of contaminants, such as chlorides for initiation, is low enough to observe the phenomenon even in continental environments [44]. The influence of contaminants on the

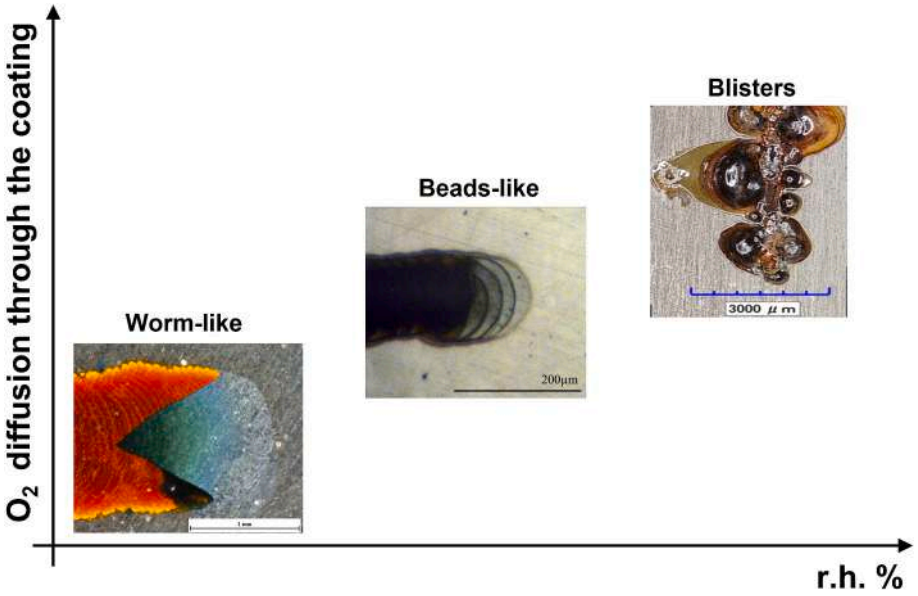

Fig. 2. Instances of coating delamination vary depending on the oxygen availability, and relative humidity of the surrounding environment. (Adapted with permission from Ref. [26, 27, 40]).

Table 2
Natural and artificial environments in which FFC has been detected.

Test	Relative humidity (%)	T (°C)	References
Natural exposure*,§,†, ‡	–	–	[28]
Humidostatic	60–95	T_{room} - 40	[14,15,33,34,57]
Cyclic	40–100 cyclic	T_{room} - 35	[18,39,40]

Exposure sites: *Marine: Key West (Florida USA), Lyon Arboretum (Hawaii USA), Waipahu (Hawaii, USA), Kilauea Volcano (Hawaii USA), §Suburban: Columbus (Ohio USA), †Rural: Ewa Nui (Hawaii USA), ‡Industrial: Campbell Industrial Park (Hawaii USA).

filiform delamination of organically coated steel has been extensively examined by Koehler [38] and Williams et al. [17]. Group (I) salts such as NaCl, KCl, and CsCl play a role in FFC initiation during the initial stages of the liquid environment formed at the interface near a damaged area. The ions derived from these salts exhibit varied actions and evolve through different stages. Anions are noted to participate in reactions throughout the entire propagation [18,26], while the role of cations is confined to the initial phase of the mechanism. Their impact is primarily associated with migration to various active spots where anodic and cathodic reactions transpire, thereby balancing the electrostatic ionic charge. Further details on the initiation mechanism will be discussed in the subsequent section.

The role of oxygen is closely tied to the integrity and permeability of the coating through corrosion products. When a scratch is present in the paint, oxygen tends to preferentially follow the paths created by the damaged area, making any potential delamination event more likely to initiate in these vulnerable spots [45–48]. Throughout propagation, the damage remains the primary source of oxygen for oxidation activity in the thread, flowing along the tail through the permeable and loose deposits of corrosion products. Studies have demonstrated that the fraction of species required to sustain the FFC's reactions passing through the intact polymeric layer is negligible in the case of a growing filament from a macro-defect. However, this minor flux might be adequate to support the propagation, influencing the kinetics and morphology of the phenomenon [26,27].

As previously mentioned, the progression of the corrosive event hinges on its initiation conditions, particularly the nucleation site responsible for supplying the necessary ionic species. Conventional corrosion tests on painted metals typically utilize longitudinal scratches [49,50]. Conversely, two primary scenarios arise in real-world applications: spot defects in the paint and cut edges. Moreover, the type of initiation feature can significantly impact the morphology of the propagation. The "V-Shape" morphology of the head or the linearity resulting from gradients in species supply [26], particularly oxygen, strongly influences the development of FFC throughout its propagation and delamination failure.

In addition to the previously mentioned factors, given the electrochemical nature of the involved reactions, the temperature is anticipated to influence the kinetics of reactions [51–54], the concentration of species in the electrolytes formed at the interface [44], and the chemical-physical properties of the paint [55,56]. Nevertheless, temperature might pose the most challenging parameter to consider in the study of painted metal corrosion, as it is intricately involved in multiple competitive mechanisms [41,51].

3. FFC knowledge: Historical background

Since Sharman's initial observation of FFC on painted iron in 1944 [1], various models of the underlying mechanism have been proposed over the decades. While some models share commonalities, others diverge, reflecting differences arising from reliance on morphological observations, rudimentary analyses, and assumptions. These hypotheses, although well-formulated, often lack robust experimental verification or disproof, primarily due to challenges in studying a phenomenon occurring beneath an organic layer. The presence of the coating has posed a significant barrier to obtaining information on electrochemical activity at the metal-paint interface. Nevertheless, certain consistent inferences about FFC features have been drawn:

i. Once the filament is well-developed from the defect, corrosion evolution involves two spatially separated electrochemically active sites: the anode and cathode. [14,24,33,38,41,58]
ii. The primary influencing factor driving thread propagation is the differential aeration between the front and back. [15,22,26,27,33]
iii. Contaminants' presence plays a role in the initiation stage, and these can migrate along the filaments during growth. [17,18,26,38]
iv. Some localized alkalinization and acidification are present in the corroding interfacial environment. [14,24,57]

However, divergent models highlight crucial points of contention:

i. The location of anodic and cathodic sites, as well as the electrochemical nature of the leading front where delamination occurs.
ii. The primary path for oxygen and water to reach the reaction sites.
iii. The existence of an active outpost preceding the filament during its propagation.

The first mechanistic interpretation of FFC, recognizing initiation and driving mechanisms, was proposed by Van Loo et al. in 1953 [28]. While their model suggested the formation of initial anodes at the exposed metal-paint junction, this theory was later disproved by Williams and McMurray fifty years later [17]. However, the propagation model based on the differential aeration between the thread's front and back parts remained valid. This study identified relative humidity thresholds above which radial blistering preferably occurs (~95 %). Consequently, FFC was defined as a corrosion event determined by exposure conditions rather than the characteristics of the coating or substrate, as it is observed in various protective systems. The discussion on the causes of the "V-shape" morphology remains unresolved until this point.

The growing interest in FFC was evident with the publication by Slabaugh and Grotheer [34] just one year later Van Loo et al. They presented the initial approximate measurement of the pH of the electrolyte at corrosion sites, detecting alkalinization (pH 12) in the exposed filament using indicator paper. However, no distinction between different reaction sites was recognized. Emphasizing the presence of Fe (II) and Fe(III) in corrosion products as crucial, they identified only Fe (II) in the green head. Consequently, they proposed that further iron oxidation to Fe(III) might occur at the junction between the head and the brown tail. A humidity threshold (65 %) was found necessary for FFC, linked to the need for water migration toward active sites. Others observed this threshold at lower values (50 %) [35]. Despite initially attributing this fact to species permeation through the organic layer by osmosis or capillarity, later studies established that the filament itself serves as the primary path for species needed for the reaction, rendering coating permeation marginal [14,26,27]. The discussion also explored the possibility of observing the "V-shaped" border between the head and tail due to the oxygen gradient capable of oxidizing Fe(II) to Fe(III) in the orthogonal direction of propagation, where lower oxygen concentration at the center could delay oxidation compared to the edges.

In 1977, Koehler [38] conducted a study focusing on the role of contaminants in the degradation of organically coated steel, specifically examining the influence of different salts on the morphology of filiform corrosion with various paint types such as epoxy, alkyd, and phenolic-based paints. The investigated salts include sodium chloride, sodium sulphate, ammonium sulphate, potassium chloride, and potassium sulphate. It was observed that sulphates produced finer corrosion filaments

compared to chlorides. The green head was found to contain chlorides, suggesting their migration through the tail via electrochemical transport. Koehler presented a model placing both corrosion semi-reactions in the leading head, a rearrangement of previously published models. Although the manuscript did not introduce new experimental evidence on the mechanism, Koehler noted a peculiar feature later unfolded and rediscovered 25 years later by Williams and McMurray [17]. Koehler reported the development of a "detachment halo" circular-shaped around the coating defect where salts were placed, categorizing it as cathodic disbonding caused by the strong bases formed by potassium and sodium.

In 1983, Ruggeri and Beck conducted a comprehensive review of filiform corrosion [14]. Beyond summarizing all available information up to that year, they delved into the role of the tail and deposited corrosion products in supporting the reaction. Theoretical calculations led them to observe that the oxygen permeating a typical polymeric coating might be sufficient to sustain FFC reactions. However, they noted that if this were the case, a symmetric cell would form instead of the directional filament growth observed. Moreover, considering the dehydration of $Fe(OH)_3$ to the presumed most stable form of iron oxide, Fe_2O_3, in the tail leads to volumetric restriction, resulting in an expected porous tail. This porous tail is assumed to be the primary pathway for oxygen and water from the defect to the FFC front. Ruggeri and Beck assert that this directional path is the main reason for the separation of anodic and cathodic sites and the stable linear growth. The "porous tail model" based on the diffusional process inside the filament head, designs the portion right behind the "V-shaped" border as the cathodic sites.

Over the years, various authors have scrutinized and critiqued the aforementioned models, proposing alternative theories. Notably, Funke [58,59] challenged the notion of the anodic nature of delamination at the head front, suggesting instead that cathodic disbonding drives the head's advancement. Funke's model revolves around the formation of a cathodic site at a distance ahead of the filament front. According to his perspective, the filament grows through the production of hydroxyl ions, leading to paint delamination owing to the alkalinization of the interface. This cathodic region is posited to develop until it merges with the filament front, allowing another separated cathodic site to form ahead. However, Ruggeri and Beck [14] contested Funke's theory, asserting that the high resistivity of the paint precludes the existence of an ionic current flow through the coating or at the metal-paint interface in the hypothesis of a distant leading cathodic site. They argued that, due to the lack of observed paint detachment preceding the filament head, there is insufficient aqueous layer at the interface to enable ionic movement through this path.

The models from the '80s lacked certain experimental evidence, leaving crucial questions unanswered and discrepancies among them unresolved. Significant progress in understanding FFC mechanisms for coated steel, aluminum, and magnesium alloys was achieved in the next century, particularly through the works of Williams et al. [11,16,17,27,60] and Stratman et al. [22,61–63]. These studies introduced the use of techniques like SKP and SIMS (Secondary ion mass spectrometry) and innovative experimental setups for collecting measured data. The subsequent section outlines the outcomes of recent studies, updated models, and remaining open questions in this field.

4. Recent advances

The initiation mechanism of filiform corrosion is acknowledged to hinge on the osmotic effect at a coating defect in the presence of soluble salts, leading to local liquid aggregation [11,14,15,34]. The phenomenon unfolds in two distinct stages. Initially, the exposed steel portion undergoes anodic dissolution of iron directly exposed to the atmosphere or electrolyte. Simultaneously, reduction activity develops around the anodic region, causing the initial delamination of the coating through the expanding cathodic front. During this phase, cations resulting from the solubilization of contaminant salts migrate toward the edges of the active region to counterbalance the negative charge of hydroxyl anions released by oxygen reduction at the cathodic front (Fig. 3b). This migration beneath the paint creates an alkaline liquid film. The presence of the initial cathodic area is evident in Fig. 3e, where the paint, loaded with 1 wt% of cresolphthalein, undergoes a color change from non-colored to purple in the pH range of 8–9.8. Concurrently, in the anodic site, the increasing deficiency of cations is promptly filled by iron cations (Fe^{2+} and Fe^{3+}) produced through steel dissolution. Consequently, iron hydroxides form, and their low solubility [64] prevents the movement of iron cations within the surrounding electrolyte. Once the cations from contaminants (such as Na^+, and K^+) are depleted at the early detached interface, the cathodic expansion halts, and a switch in the reaction role is observed [17].

During the second phase, the anodic activity takes precedence at the delamination front, now governed by an anodic undermining process. In these reversed scenarios, chloride anions migrate from the defect to the leading [60]. The interfacial liquid becomes increasingly enriched with anions from the cathodic reaction (mainly oxygen reduction) and cations from the anodic one (iron oxidation). Additionally, the oxygen gradient induces the formation of localized cathodic and anodic sites. Differential aeration underlies filament formation, as the salt concentration contributes to the reduction in oxygen solubility at the filament front, leading to a lower concentration compared to the rear part [15,24,27]. These findings are primarily derived from SKP and SIMS investigations, particularly in the case of polyvinyl butyral (PVB) coated mild steel. A dark halo around the scratched zone is evidence of the initial cathodic disbonding, and its expansion halts once FFC is present, aligning perfectly with the two-phase model proposed by Williams et al. [17]. Fig. 4 illustrates an example of a stationary cathodic halo around a longitudinal scratch while FFC progresses over time under humidostatic conditions (40 °C and 80 % r.h.) [26]. It emerges during the phase of salt spray contamination and appears to exhibit stability irrespective of the duration of exposure under humid conditions. Notably, in accordance with the universally accepted linear growth velocity of filaments, a slight reduction (15 %) in growth rate is observed once the filaments extend beyond the halo region and advance into the intact interface [17]. This observation serves as evidence for a diminution in coating adhesion, attributable to the initial phase in the FFC process. Furthermore, enhanced adhesion contributes to a deceleration in the corrosion creep.

Once the filament is fully developed, the propagation is believed to be responsible for the coating delamination through anodic undermining processes involving the migration of chlorides and sulphates anions to the front region and iron cations toward the rear portion of the head and the tail, where the cathodic reactions occur.

In a recent publication [24], a map depicting the distribution of electrochemical activities along filaments was presented, utilizing Scanning Vibrating Electrode Techniques (SVET). Fig. 5 displays SVET maps of samples featuring artificial defects introduced through the coating. These defects are located at the head Fig. 5b and in the tail Fig. 5d. The scanning process commenced approximately 3 min after the perforation stage and roughly 1 min into immersion in the naturally aerated test solution. Distinctly, positive ionic currents were measured in the green-colored head, and negative currents were observed in the brownish tail. These signals can be qualitatively attributed to the corresponding anodic (positive) and cathodic (negative) corrosion reactions persisting beneath the coating. Notably, these reactions were still evolving despite the time elapsed between the creation of the defects and the actual scanning measurement. The authors concluded that the entirety of the green head encircled within the designated "V-shape" border alongside brown corrosion products, was demonstrated to exhibit anodic behaviour. Notably, the intensity of this activity appeared to be more pronounced in the darker posterior portion compared to the leading halo. This observation contradicts certain models found in the literature that propose a cathodic delamination outpost; instead, the

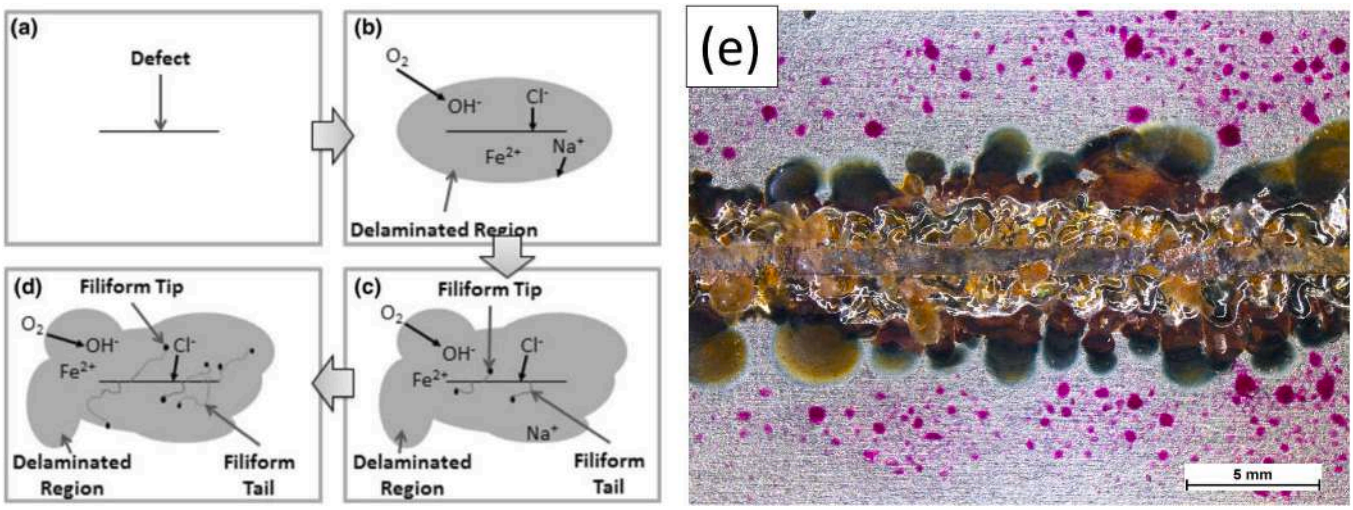

Fig. 3. FFC initiation mechanism proposed by Williams et al. [17] for defected organic coated steel with group (I) salts contamination (a-c) (Adapted with permission from Ref. [17]). Optical image captured on acrylic-coated steel after one day of humidostatic condition (80 % r.h.) following 5 h NSST contamination (e). In this case, the paint was loaded with 1 wt% of cresolphthalein which changed from non-colored to purple in a pH range of 8–9.8. A darker-colored halo is visible around the scratch and several purple-colored spots are present testifying to the cathodic activities in the first phase of FFC (Adapted with permission from Ref. [18]). (For interpretation of the references to color in this figure legend, the reader is referred to the web version of this article.)

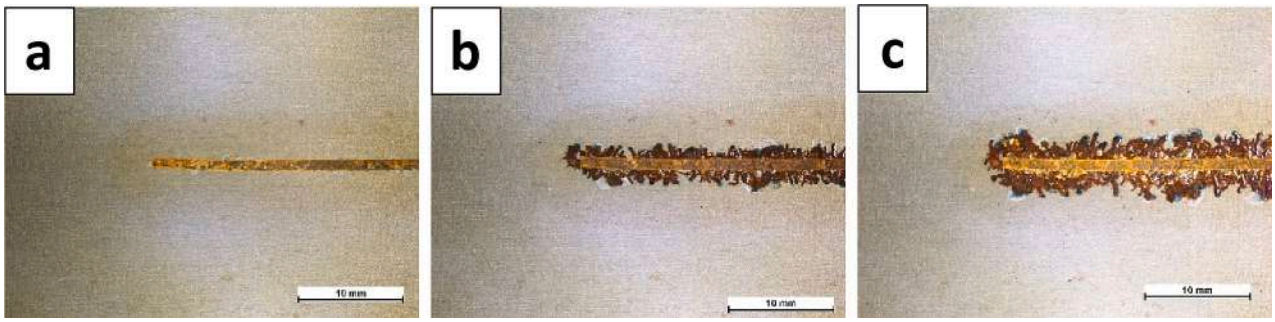

Fig. 4. Images comparison of samples after 70 (a), 600 (b), and 1000 (c) hours of humidostatic aging (40 °C and 80 % r.h.). Adapted with permission from Ref. [26].

delamination front was unequivocally identified as having an anodic character. Moreover, in this study, the role of the tail was unrevealed: the entire length of the brown filament thread displayed electrochemical activity conducive to the reduction of oxygen, effectively serving as the cathodic site. This finding supports the notion that the brown filament tail plays a crucial role in filament propagation.

At the metal-paint interface, the species' movement is driven by a potential/concentration gradient between the two active sites in the head [26]. A differential aeration cell is created due to the easy diffusion of oxygen through the tail to the tip of the filament. The leading portion of the head is considered to have a lower concentration of oxygen, influenced by restricted availability, high ionic strength, and lower pH [24]. Oxygen supply to the reaction sites is crucial for the filament's shape development. Watson et al. [27] demonstrated that the amount of oxygen permeating through the coating is sufficient to sustain filament propagation. However, in the case of a macro-defect (the most common situation), oxygen-supporting filament propagation is supplied from the porous tail, resulting in a higher concentration in the back of the head compared to the front (schematized in Fig. 6).

This outcome has been corroborated by Cristoforetti et al. in a subsequent publication [26]. Furthermore, the referenced study establishes the significance of oxygen supply distribution in the formation of the characteristic "V" border between the green and brownish corrosion products. The availability of oxygen at the active filament site situated in the head not only influences the driving force for filament propagation but also plays a crucial role in determining the morphology of the filament head. The primary source of O_2 was altered from the tail pathway to paint permeation mode. In this experiment, FFC was initiated and promoted on acrylic-coated carbon steel panels. After approximately 500 h of testing, during which the average filament length measured about 6 mm, the scratch was sealed using epoxy resin to observe the progression of FFC in the absence of oxygen flux through the tail (Fig. 7b). Interestingly, when the oxygen supply from the tail was nullified, the greenish compounds in the "V-shaped" head transitioned to brownish corrosion products, resembling the tail (Fig. 7c). Moreover, a new anodic head emerged with a distinctly different morphology, losing the characteristic "V-shape" and the well-defined edge between the head and the tail (Fig. 7d). The greenish compound-rich portion of the head exhibited a more circular blister-like appearance. This observed behaviour is attributed to the change in the main source of oxygen once the scratch is sealed through the paint. The second growth stage, characterized by a radially symmetric oxygen source from the atmosphere through the paint, does not exhibit the peculiar "V-shaped" head due to the absence of an oxygen gradient in the propagation direction. The results support the hypothesis by Slabaugh and Grotheer [34] regarding the diffusion gradient attributed to the shape of the corrosion cell's roof. However, the experimental outcomes reported in Fig. 7 contrast with this interpretation, indicating that the primary oxygen concentration gradient affecting iron oxidation comes from the tail path rather than through the coating. Therefore, the existence of a gradient in the oxygen flux in the tail is presumed due to the synergistic effect of corrosion product permeability and paint detachment.

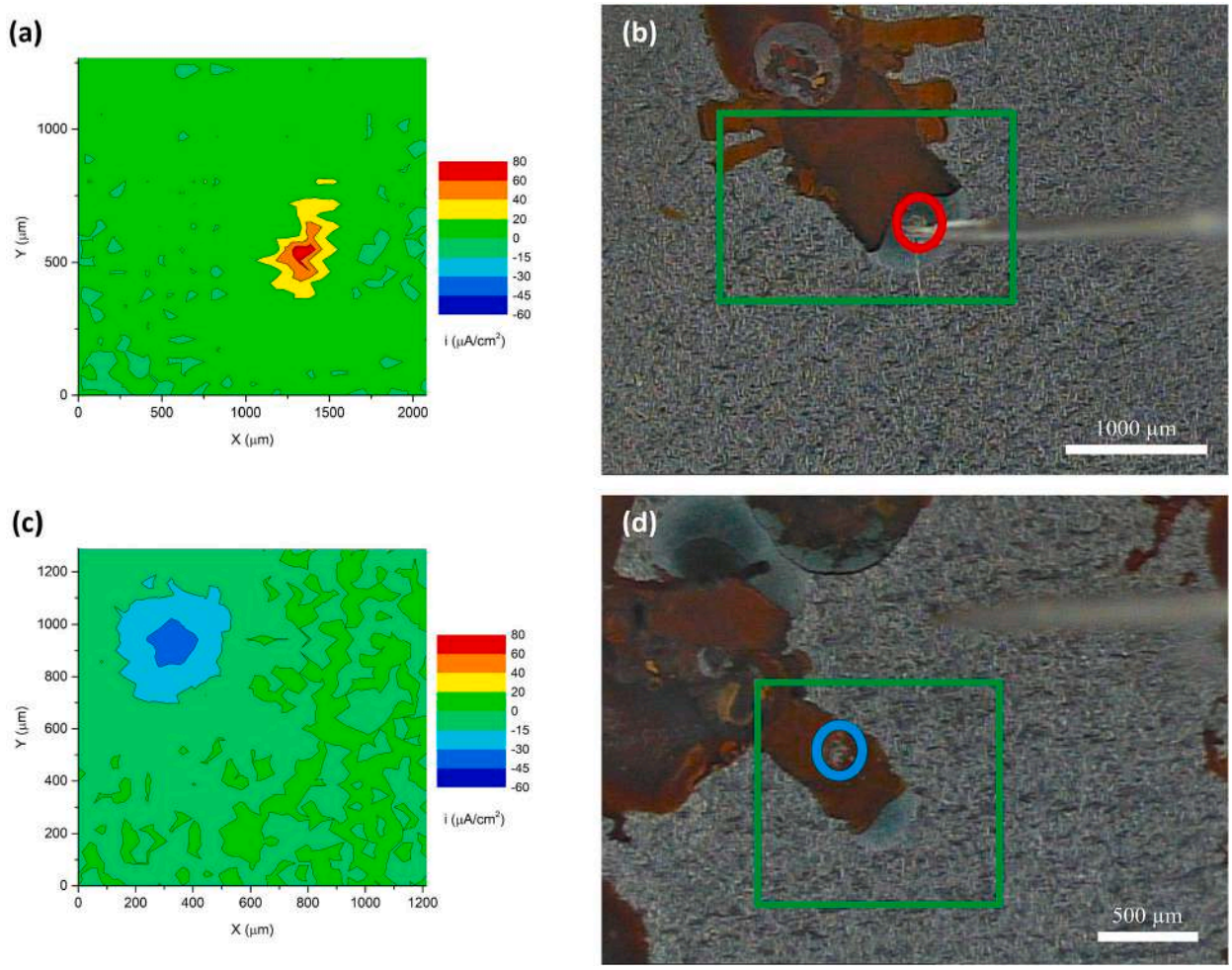

Fig. 5. Ionic current map in microamperes per square centimeter (μA/cm^2) was acquired through Scanning Vibrating Electrode Technique (SVET) (a and c). Accompanying this, an optical micrograph is provided for the surveyed square area, illustrating perforated circular defects. These defects are distinctly positioned in the brown-colored tail, the green-colored leading head, and the pristine uncorroded surface (b and d). Adapted with permission from Ref. [24]. (For interpretation of the references to color in this figure legend, the reader is referred to the web version of this article.)

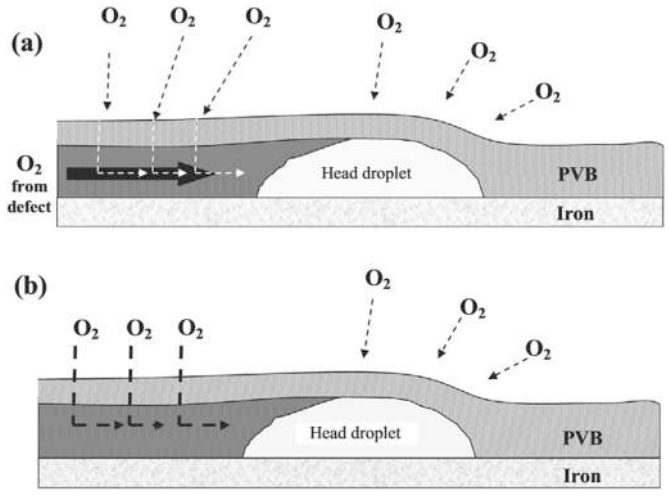

Fig. 6. Schematic representation of FFC highlighting (a) oxygen availability when a defect in the coating is present, and (b) sources of oxygen when any defect is not present. In (b) sufficient concentration gradient is maintained by the oxygen permeating through the coating. Adapted with permission from Ref. [27].

The propagation takes place when iron undergoes oxidation in the anodic region according to reaction 1, and the released cations move through the electrolyte, reaching the cathodic region where reaction 2 occurs. At this point, the iron cations further oxidize to Fe^{3+} due to the presence of oxygen at the cathode, further supporting local alkalinization. The ferric ions rapidly combine with the OH^- anions (reaction 3). Next, dehydration of the corrosion products takes place in the tail region according to reactions 4 and 5. The change in the iron oxidation state corresponds to the shift in color between the head and the tail, where iron compounds deposit as brownish clamshell marks.

$$Fe \rightarrow Fe^{2+} + 2e^- \quad (1)$$

$$4Fe^{2+} + O_2 + 2H_2O \rightarrow 4Fe^{3+} + 4OH^- \quad (2)$$

$$Fe^{3+} + 3OH^- \rightarrow Fe(OH)_3 \quad (3)$$

$$Fe(OH)_3 \rightarrow FeOOH + H_2O \quad (4)$$

$$Fe(OH)_3 \rightarrow \frac{1}{2}Fe_2O_3 + \frac{3}{2}H_2O \quad (5)$$

During FFC, in the case of painted steel, the electrochemical reaction in the filament leads to the formation of regions with significantly different pH values of the electrolyte. Besides the ancient measurement by litmus paper in the corrosion products [14,34] along the tail, a recent

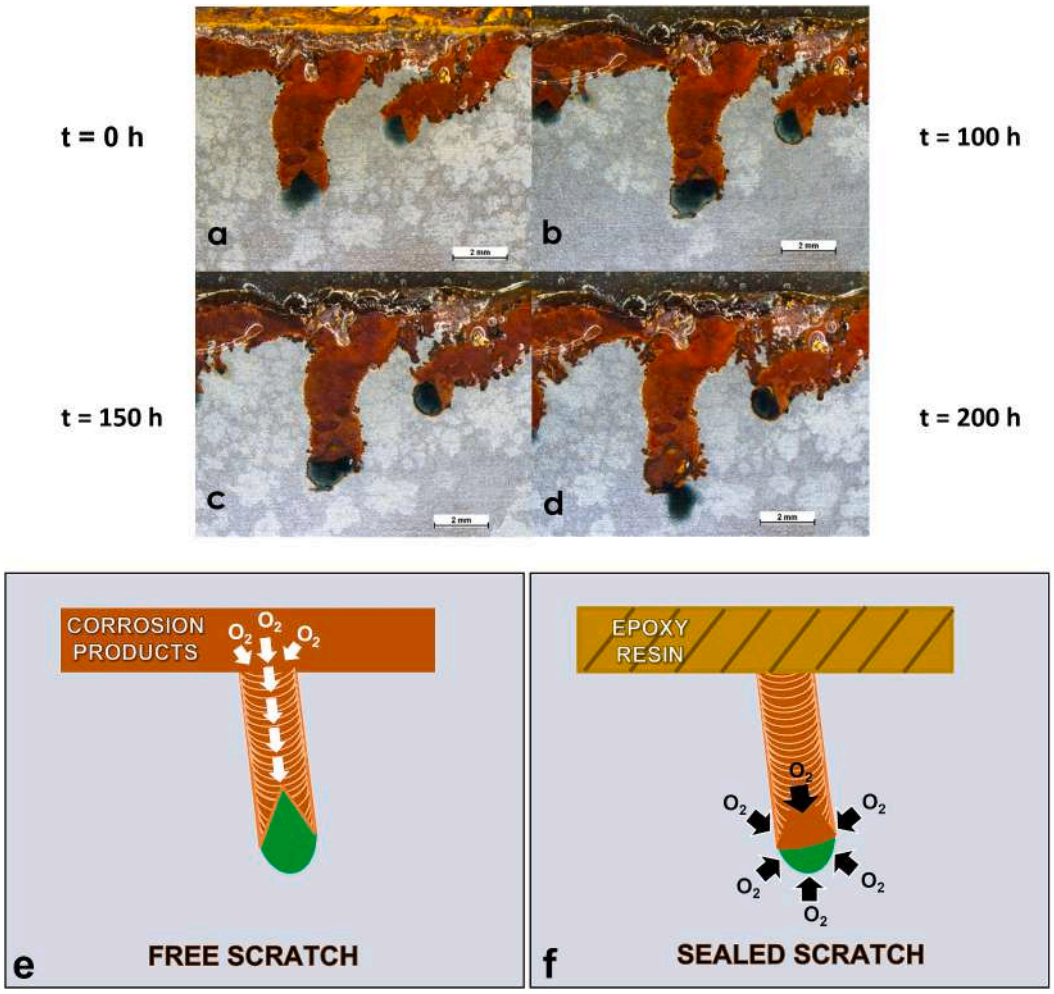

Fig. 7. Evolution of FFC morphology and "V" shape disappearance after the scratch sealing from time zero (a) to 200 h (d) of 80 % humidostatic condition at 40 °C. Pictures (e) and (f) show a schematic view of the oxygen source before and after the scratch sealing. Adapted with permission from Ref [26].

publication [24] reported about an in-situ pH measurement at the interface by antimony electrode-based micropotentiometry. They obtained a value of alkalinity in the interfacial region of 10.5 along the tail, while the environment of the leading portion coinciding with the green rust is characterized by a slight acidification (pH 4.5). These outcomes furtherly enhance the theory of propagation based on the spatial distribution of the anodic and cathodic reaction. This distinctive pH distribution results in the "V-shaped" head with a clear boundary between the head and the tail (see Fig. 1), highlighted by the color contrast of different Fe^{n+} containing compounds in the two regions. According to the literature, the head exhibits a metastable greenish mixture of Fe(II) and Fe(III) compounds, known as "green rust" (GR), studied since the work of Bernal et al. [65] in 1959 and more recently classified as fougerite ($Fe_2^{+4}Fe_3^{+2}(OH)_{12}[CO_3]\cdot 3H_2O$) [28,66–68]. GR, exhibiting stability at the leading edge of the filament due to a reduced oxygen concentration, underwent precipitation as amorphous iron oxide upon the filament's progression and exposure to oxygen [28]. The green rust formation was initially observed in the presence of sulphates, leading to the development of Fe(II)–Fe(III) hydrosulphate [69,70]. Later, attention shifted to the role of chlorides in green rust formation, resulting in Fe(II)–Fe(III) hydroxychloride [71]. Bernal's XRD studies classified these compounds as GR1 and GR2, corresponding to hydroxychloride and hydrosulphate, respectively [65]. GRs are complex and abundant intermediate corrosion products in iron degradation in various environments, such as the atmosphere, liquids, or soil. In the tail, where iron undergoes further oxidation and oxygen availability is higher, the corrosion products are believed to be primarily hematite ($Fe_2O_3\cdot xH_2O$) [27]. Moreover, when the corrosion products dehydrate to Fe_2O_3, they form the expected porous tail, as the volume reduction from 97 % to 55 % increases the free space at the interfacial occupied volume [14].

Cambier et al. [28] utilized Raman spectroscopy to assess the formation of steel corrosion under organic coatings, specifically focusing on FFC during outdoor exposure. Within this investigation, Raman spectra corresponding to the crystallization stages of akaganeite ($FeO_{0.833}(OH)_{1.167}Cl_{0.167}$) were discerned in the restricted electrolyte beneath the coating in the leading part of the filaments (Fig. 8). Akaganeite is known to develop in environments with elevated chloride concentrations [72,73], while green rust remains stable in low-oxygen electrolytes when the $[Cl^-]/[OH^-]$ ratio surpasses a certain threshold. Notably, green rust precipitates from chlorine-containing GR1 when chloride species are present in the absence of sulphate or carbonate. It is important to note that magnetite and goethite can also emerge as alternatives to akageneite [28,74]. Goethite tends to precipitate in sulphate-rich environments. However, the Raman spectrum did not indicate the presence of sulphate beneath the coating, introducing uncertainty regarding the role of sulphate in the corrosion mechanism. Furthermore, the investigation revealed that the iron oxides constituting the filament were not contingent on the specific field site.

Beyond the observed morphology reported thus far, depicted in Fig. 1, where the head front gradually merges with the pristine coating and the propagation is continuous, another phenomenon may be observed. Under specific conditions related to coating permeability to

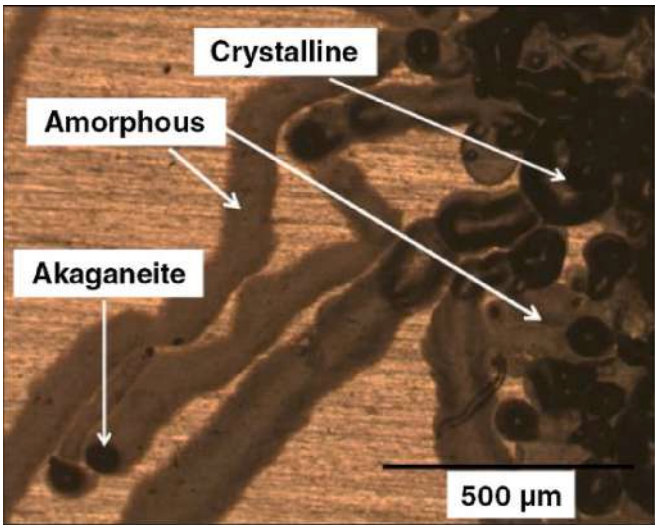

Fig. 8. Iron oxides found by Cambier et al. [28] by Raman spectroscopy on a PVB coated sample exposed outdoors. Adapted with permission from Ref. [28].

oxygen and external partial pressure, continuous growth may be substituted by a saltatory mechanism, resulting in a so-called "bead-like" morphology [19,28], as shown in Fig. 9c-d and Fig. 10. In this case, upon observing the evolution over time, the advance appears as a step-wise mechanism rather than a smooth one. The presence of a dark annulus at the edge of the head front is detected, and the propagation consists of the formation of a further semicircular annulus at a constant distance from the previous one. The typical "V-shape" border is no longer clearly identifiable, along with the linearity of the filament. Watson et al. [27] extensively investigated this phenomenon, especially in relation to the variation of the oxygen partial pressure in the environment surrounding the coating over the defect and its ratio to the one experienced by the open defect. They concluded that when the oxygen partial pressure over the coating is above a certain threshold, saltatory growth occurs through the formation of a cathodic ring placed at the leading edge of the head. Subsequent rings develop over time with a constant frequency. The cause of this cathodic activity happening at the front lies in the high amount of oxygen reaching the interface, creating an oxidizing environment leading to the deposition of iron hydroxide, the main constituent of the dark ring (Fig. 9a-b). This fact is proven by the disappearance of the annular hydroxide deposition when O_2 is removed from the atmosphere in contact with the coating covering the filament, thanks to the experimental setup specifically built by Watson et al. In these

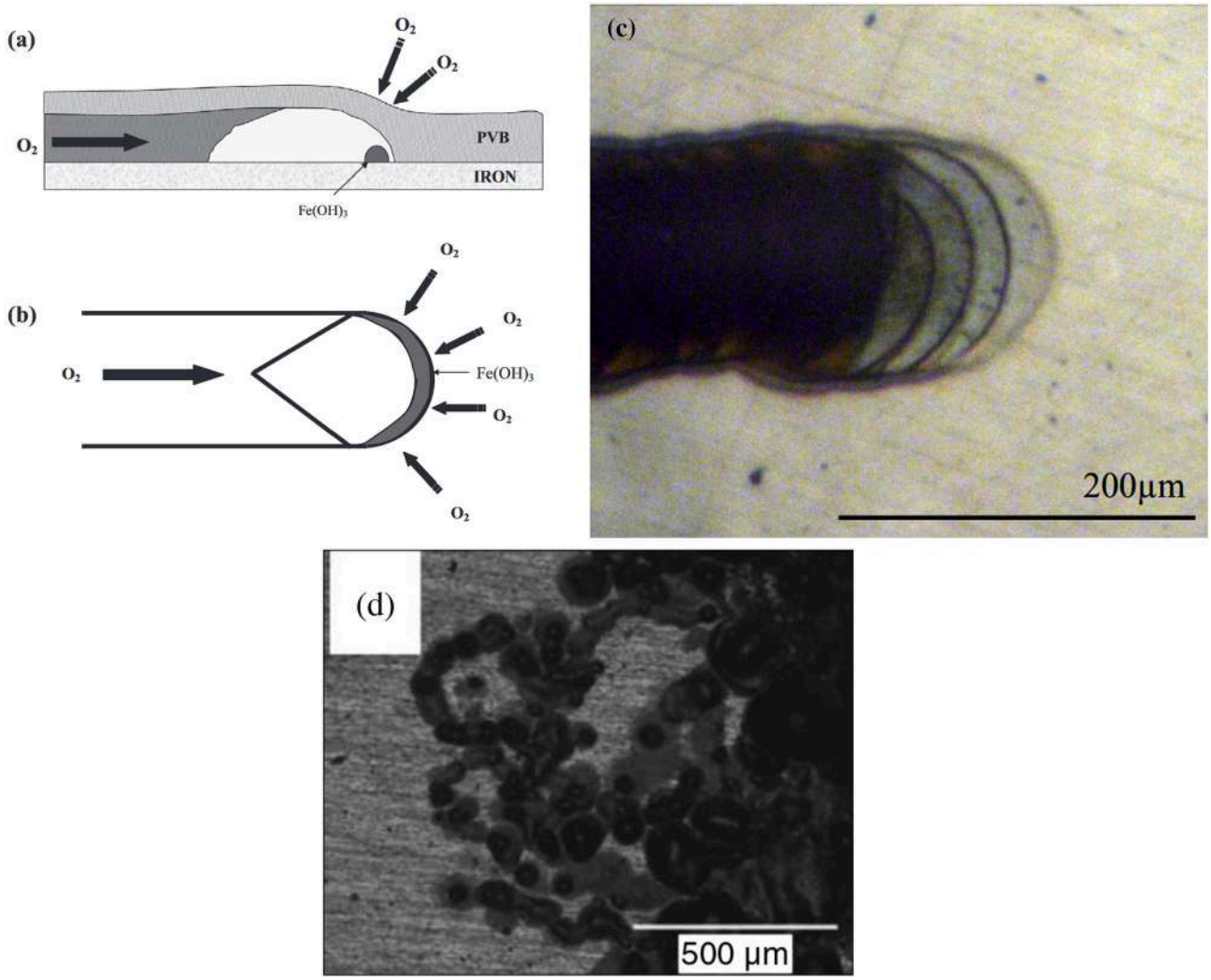

Fig. 9. Schematic view of (a) cross-section and (b) top-view of a filament showing the mechanism of the formation of an anterior ring (adapted with permission from Ref. [27]). (c) is an optical image taken on a filament growing by a saltatory mechanism in a PVB clear-coated steel substrate (adapted with permission from Ref. [27]). (d) reports a typical "bead-like" corrosion event developed outdoors (Waipahu, Hawaii). Adapted with permission from Ref. [28].

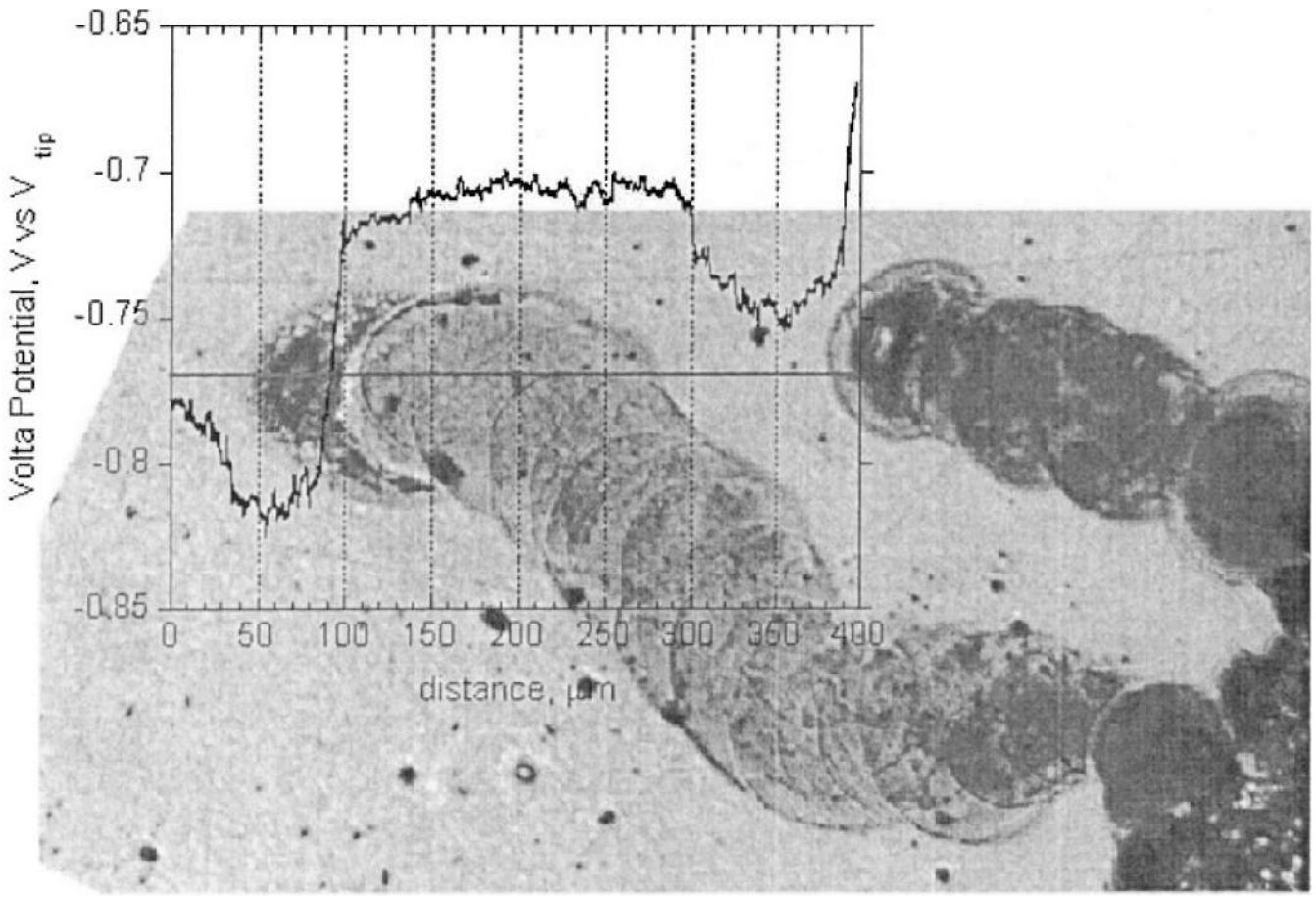

Fig. 10. SKPFM line scan along the filament developed on an epoxy-coated carbon steel substrate. The combination with the optical micrograph image highlights the different electrochemical activities in the analyzed region. Adapted with permission from Ref. [19].

dummy experimental conditions, the only oxygen is coming from the defect through the tail, reaching the head. Since other authors reported similar morphologies in standard aging conditions (i.e., in 93 % r.h. after chlorides contamination [19]) with other coating systems (i.e., epoxy or acrylic-based), a further step in the discussion could be made. Under a combination of oxygen permeability through the coating and external atmospheric parameters (humidity, temperature, and atmospheric pressure), the formation of iron hydroxide deposits is favoured thanks to the O_2 enrichment in that region. The reason behind the annular distribution around the head is suggested to be the finer thickness of the head droplet. Furthermore, the supposed cathodic activity is explained to periodically end because of the absence of cations in the head capable of providing long-range ionic conduction to sustain proper cathodic disbonding [27]. The actual role of the promoter or retarder of FFC growth introduced by this cathodic ring is still unresolved, but the possibility of encountering this phenomenon is fully accepted. Leblanc and Frankel [19], using a Scanning Kelvin Probe Force Microscope (SKPFM), underline the presence of an anterior cathodic region in a growing filament's head. The carbon steel samples analyzed in this case were epoxy-coated and showed a "string of beads" morphology, as reported in Fig. 10. They pointed out that the green-colored head possesses a low potential with respect to the tail, but the poor imaging contrast combined with the small difference left the actual location of the main anode and cathode unclear. In this work, all reactions are assumed to occur in the leading head; however, the authors stated the uncertainty of this outcome of their low-resolution SKP measurements. In a groundbreaking study, Senöz and Rohwerder [75] pioneered the real-time monitoring of FFC through high-resolution SKPFM. Although their investigation focused on aluminum alloy, its findings bear significance for steel as well, as they align with the findings of Lebalnc and Frankel [19] regarding the localization of anodic and cathodic regions. Additionally, the study sheds light on the influence of intermetallic particles on corrosion propagation and rate, as well as their impact on alterations in potentials and coating adhesion.

5. FFC prevention strategies

A comprehensive strategy for corrosion mitigation, particularly addressing FFC, involves ensuring robust paint adherence to the metal surface [62,76–78]. For instance, Harun et al. [79] reported on the enhanced wet and dry adhesion given by a steel surface modification with 3-glycidoxypropyltrimethoxy silane resulted in a notable reduction of the delamination rate for an epoxy coating, achieving a threefold decrease. Employing pretreatments before the painting process can enhance both the compatibility of the metal with the paint and its resistance to moisture [80]. However Marsh et al. [81] observed that certain treatments significantly improved adhesion, while others notably enhanced resistance to corrosion and/or delamination, but these phenomena were not always correlated. Reducing the number of defects in the coatings and adequately protecting cut edges are crucial practices [82–84]. It has been noted that improper paint application and variations in coating thickness may contribute to FFC [15]. While penetrative defects are a primary source of concern, low-permeability coatings are generally preferred. Thick and multilayer coating systems can reduce the likelihood of heterogenies serving as initiation sites for FFC. Consequently, pigment loading plays a significant role and acts as an additional variable influencing FFC susceptibility.

An approach to preventing corrosion involves modifying the

aggressive environment, achieved through pH adjustment, reduction of oxygen availability, or the introduction in the coatings of chemical species such as inhibitors capable of slowing down the corrosion process. Various substances exhibit corrosion-mitigating properties, categorized based on their operating mechanisms. These include physical adsorption and chemical interaction, overpotential increase in cathodic and anodic reactions, sheltering effect against oxygen reaching the metallic surface, and favouring metallic passivation [85–87]. Implementing corrosion prevention through environmental conditioning and the judicious use of inhibitors based on these mechanisms offers a versatile and effective means to combat corrosion-related challenges. Also, the metallic surface modifications and treatment prior to the painting could enhance the resistance to coating delamination.

In this context, conversion coatings (CCs), typically inorganic layers improve the corrosion susceptibility and the adhesion at the steel paint interface. They can increase the surface roughness, modify the surface chemistry, and increase the surface energy level [80]. Moreover, the deposited layer acts as a barrier against the electron transfer between anodic and cathodic sites [88,89]. Numerous studies have investigated the impact of CCs on mitigating FFC in organic-coated aluminum [37,90–92]. However, to the best of our knowledge, there is a lack of specific research focused on treated steel substrates. Cristoforetti et al. [93] recently reported the effect of commercial steel CCs, such as trivalent chromium-based and phosphating, on FFC susceptibility. They found that phosphating significantly enhanced the resistance to filaments initiation and propagation, while the contribution provided by trivalent chromium was less visible in the testing conditions considered in the study (acrylic-coated steel samples in a humidostatic environment 80 % r.h. at 40 °C).

In the context of CCs, in the existing literature, considerable efforts have been directed toward leveraging some eco-friendly materials such as Layered double hydroxide (LDH) as a surface treatment or a thin coating applied prior to the organic covering. This approach has proven successful, especially for aluminum [3,94–96] or magnesium alloys [97,98], where the surface actively participates in the synthesis, resulting in a well-adherent and protective inner layer. However, achieving satisfactory results on steel remains challenging. Recent studies have endeavoured to develop hydrotalcite-based coatings on steel through in-situ growth [99–101]. Various compositions, including those involving iron ions (MgFe) or not (MgAl), have been explored. While these systems demonstrate corrosion protection in concrete environments, their limited adhesion, attributed to poor compatibility with the substrate and ceramic material, poses challenges for their application in atmospheric corrosion protection or in conjunction with organic coatings.

In addition to surface treatments, incorporating corrosion inhibitors into the coating is a potential solution. Once activated or released, these inhibitors can interact with the metal-paint interface, potentially forming a protective film on the surface or creating a passivating environment [37,102,103]. The effectiveness of inhibitors relies on various factors, including their stability, activation, pH of the environment, oxidative state of the metal, and interactions with other chemical and microbiological species [104]. Consequently, a thorough understanding is crucial to tailor an appropriate protective system. In the context of FFC, several inhibitors have been investigated to counteract the degradation of painted steel. For instance, Peng et al. [105] achieved success with a 20 wt% addition of rare earth carboxylates, namely lanthanum 4-hydroxycinnamate ($La(4\text{-}OHcin)_3$) and yttrium 3-(4-methylbenzoyl) propanoate ($Y(mbp)_3$), in epoxy coating. In particular, lanthanum 4-hydroxycinnamate acts as a mixed inhibitor [106], effectively suppressing the initiation and propagation of FFC, as well as cathodic delamination when added to polyurethane varnish at a concentration higher than 10 wt% [36,105].

Glover and Williams [37] demonstrated the efficacy of phenyl phosphonic acid (H_2PP) in PVB, particularly above the concentration threshold of 10 wt%. Under these conditions, the authors proposed the formation of a Fe_2PP layer that acts as a barrier, preventing Cl^- adsorption onto the iron surface and reducing the observed progression rate.

Exbrayat et al. [107] incorporated Mercaptobenzotriazol (MBT) into silica nanocapsules containing a corrosion fluorescence nanosensor. In the composite coatings, which are PVB-based, MBT effectively inhibits the delamination process, leading to the absence of filament propagation as observed in the study.

Recently, poly(diallyl dimethylammonium) coumarate (polyDADMA-COU) has been evaluated and has shown promising results when incorporated into acrylic coatings at a concentration of 10 wt% [108]. This system demonstrated improved adhesion levels to the steel substrate and active corrosion protection. Potentiodynamic polarization tests revealed a maximum inhibition efficiency of 96 % while under standard testing conditions of 80 % r.h. and 40 °C after one month, coatings containing 10 % polyDADMA-COU exhibited only minimal corrosion points, with no evidence of filiform corrosion propagation, contrasting with control specimens that were fully damaged by anodic undermining.

Other candidates for this purpose are benzotriazole and benzotriazolate, which have been explored more on zinc-aluminum-magnesium coated steel [109]. It's noteworthy that the available inhibitive species specifically evaluated for an anodic undermining mechanism are limited, and further efforts are needed in this regard. A comparison of the mitigation performances achieved to date for steel substrates exploiting various strategies is provided in Table 3.

The use of inhibitors within organic coatings may pose technological challenges, including issues such as leaching or a reduction in efficiency due to interactions with the polymeric matrix, as observed with carboxylates and epoxy-based paints, leading to a decrease in the barrier performance of the coating [110]. One strategy to address these undesired effects is to incorporate inhibitor molecules into nanocontainers capable of hosting them within the coating and releasing them when activated by the evolving aggressive environment (e.g., water uptake or chloride accumulation) [111–113]. LDH anionic clays, also known as hydrotalcite, represent one of the most promising systems for this purpose. They can be utilized not only as treatment for metal surfaces before the painting stage but also as a pigment embedded in the organic coating [3,31,32,94,110,112,114,115]. This system exhibits an anion-exchange character and is suitable as an anionic inhibitor nanocontainer [110,115–123]. In addition to their ability to store and release inhibitor compounds, LDH pigments based on hydrotalcite or calcined hydrotalcite may also serve as chloride scavengers. The smaller size of Cl^- facilitates anionic exchange compared to the intercalated molecules, making this property particularly useful for FFC prevention

Table 3
Reduction of FFC propagation rate for organic coated steel by various mitigation strategies collected from the studies available in the literature.

Coating	*Inhibitor **CC	Relative humidity (%)	T (°C)	Reduction in corrosion rate (%)	References
Epoxy	*20 wt% La $(4OH\text{-}cin)_3$	85	40	99	Peng et al. 2023 [105]
Epoxy	*20 wt% Y $(mbp)_3$	85	40	85	Peng et al. 2023 [105]
Polyurethane	*10 wt% La $(4OH\text{-}cin)_3$	85	40	71	Catubig et at. 2011 [36]
PVB	*12 wt% H_2PP	95	25	76	Glover et al. 2017 [37]
Acrylic	*10 wt% polyDADMA-COU	80	40	96	Minudri et al. 2023 [108]
Acrylic	**Cr(III), Phosphating	80	40	6, 35	Cristoforetti et al. 2024 [93]

[113,124–127].

Some efforts have already been directed toward this approach, particularly in the context of FFC of organic-coated aluminum [32,128], magnesium [109], and zinc-aluminum-coated (ZAM) steel [31], employing inhibitors-doped commercial hydrotalcite. Encouraging results should stimulate increased scientific interest in this field, with a focus on overcoming the use of chromium. Wint et al. [31] proposed a model (Fig. 11) in which anionic exchange occurs during filament propagation at the metal-coating interface. In their study, acetic acid was used to initiate FFC PVB-coated ZAM-coated steel. Recent research has demonstrated the remarkable resistance of organic-coated $MgZn_2$, a predominant phase in ZAM alloys [129], against cathodic delamination, but a significantly higher likelihood of organic coating delamination occurring via anodic undermining [130,131]. For ZAM substrates, FFC could be initiated through the introduction of small quantities of acetic acid into a penetrative defect in the organic coating. Interestingly, chloride-based electrolytes (such as NaCl, $FeCl_2$, and HCl) do not consistently induce FFC on these substrates. Preferential anodic dissolution of magnesium-rich eutectic phases could create pathways within the ZAM coating, facilitating oxygen diffusion to the iron substrate. Consequently, iron exposed in the FFC tail (or at the tail-head droplet interface) forms a galvanic couple with ZAM, thereby intensifying the driving force for filament advancement. These findings underscore the complex interplay of factors contributing to the initiation and propagation of FFC on ZAM alloys [20,132].

In this context, during FFC propagation, the presence of acetate anions is driven by the electrostatic need for neutrality at the anodic site. In this scenario, carbonates intercalated into hydrotalcite particles are presumed to migrate in the delaminated volume, replacing acetates. While this example may be distant from the service conditions during atmospheric corrosion, the same principle could be applied to the release of inhibitors by pigments, also in the case of steel substrates, potentially mitigating the propagation of FFC. Moreover, the beneficial effect could be observed at the initiation stage, depending on the type of inhibitor released. However, for filiform corrosion nucleation on painted steel, the scavenger capability of hydrotalcite may be deemed ineffective, as the main role of Group I cations is demonstrated to drive the process [17].

FFC is exacerbated by rough surfaces and contaminated metallic substrates [133]. Therefore, thorough surface preparation before painting is essential for ensuring durability [134]. Special attention should be given to the sandblasting procedure, as embedded oxide particles during this process may weaken the metal-paint interface [15]. It is imperative to avoid salt contaminants at the interface, necessitating careful consideration of the storage environment for uncoated parts and the level of care in the painting plant.

The choice of an appropriate mitigation strategy should be informed by a detailed understanding of the specific degradation mechanism at play. In the context of preventing coating delamination, it is essential to consider the reactions at the extending front, as corrosion inhibition behaviour is often categorized as cathodic or anodic [135]. While some strategies may offer general metal protection irrespective of the corrosion mechanism, others are more tailored to specific phenomena such as FFC, which is cathodically nucleating and typically exhibits anodic delamination. The selection of a mitigation pathway is, therefore, contingent on the intricacies of the corrosion process.

6. Conclusions

This paper offers an in-depth exploration of the origins, processes, and preventive measures related to filiform corrosion in steel coated by organic layers.

The corrosion mechanism's review reveals a complex two-stage process influenced by coating defects, soluble salts, and electrolyte conditions. The first stage involves anodic dissolution of exposed steel, leading to cathodic delamination facilitated by the migration of cations from contaminant salts. The initial cathodic area is evidenced by a color change in the paint, and this phase is crucial for subsequent filament development. The second phase is characterized by anodic undermining at the delamination front, with chloride anions migrating to the leading edge. Filament formation is driven by differential aeration, resulting in oxygen concentration gradients.

Filament growth and morphology are influenced by oxygen supply, with the tail playing a crucial role in sustaining filament propagation. Oxygen flux through the tail affects the "V-shaped" head and the overall filament morphology. Sealing the scratch interrupts the oxygen supply, leading to changes in the head's appearance and filament growth characteristics.

The electrochemical reactions in the filament contribute to distinct pH distributions along the head and tail, influencing the formation of corrosion products. Green rust and other iron compounds are identified, with their precipitation influenced by chloride concentrations. Raman spectroscopy and in-situ pH measurements provide valuable insights into the corrosion products' composition and distribution.

Under specific conditions, a saltatory growth mechanism may replace continuous growth, resulting in a "bead-like" morphology. This phenomenon is attributed to oxygen permeability through the coating and external atmospheric parameters. The presence of cathodic rings and periodic annular hydroxide deposits suggests a complex interplay between oxygen availability, cation conduction, and filament growth.

A suitable strategy to mitigate filiform corrosion involves meticulous surface preparation, the application of low-permeability coatings, and the incorporation of tailored inhibitors. In the case of steel substrates, promising solutions include conversion coatings, and environmentally friendly smart coatings like layered double hydroxides. Understanding specific corrosion mechanisms and implementing these technologies collectively could enhance the resistance of steel surfaces to filiform corrosion.

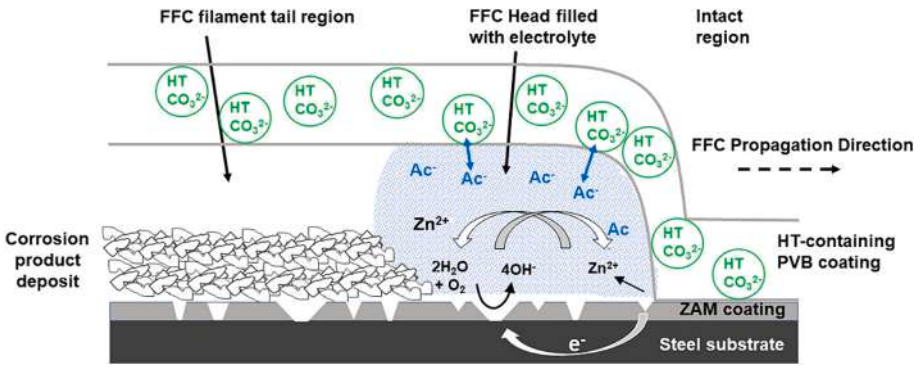

Fig. 11. Schematic representation of the mechanism of ionic exchange during FFC propagation involving the hydrotalcite pigments loaded in the coating. Adapted with permission from Ref. [31].

In summary, this updated overview contributes to a comprehensive understanding of filiform corrosion initiation, propagation, and morphology. The insights gained from this study provide a foundation for future research on corrosion prevention and mitigation strategies in coated metal systems.

CRediT authorship contribution statement

Andrea Cristoforetti: Writing – review & editing, Writing – original draft, Methodology, Investigation, Data curation, Conceptualization. **Stefano Rossi:** Writing – review & editing, Validation, Supervision, Project administration, Conceptualization. **Flavio Deflorian:** Supervision, Project administration. **Michele Fedel:** Writing – review & editing, Validation, Supervision, Project administration, Conceptualization.

Declaration of competing interest

The authors declare that they have no known competing financial interests or personal relationships that could have appeared to influence the work reported in this paper.

Data availability

No data was used for the research described in the article.

References

[1] C.F. Sharman, Filiform underfilm corrosion of lacquered steel surfaces, Nature 3890 (1944) 621–622.

[2] A. Nazarov, A.-P. Romano, M. Fedel, F. Deflorian, D. Thierry, M.-G. Olivier, Filiform corrosion of electrocoated aluminium alloy: role of surface pretreatment, Corros. Sci. 65 (2012) 187–198.

[3] M. Fedel, C. Zanella, L. Ferrari, F. Deflorian, Effect of the synthesis parameters of in situ grown mg-Al LDHs on the filiform corrosion susceptibility of painted AA5005, Electrochim. Acta 381 (2021) 138288, https://doi.org/10.1016/J.ELECTACTA.2021.138288.

[4] N. LeBozec, D. Persson, D. Thierry, S.B. Axelsen, Effect of climatic parameters on filiform corrosion of coated aluminum alloys, Corrosion 60 (2004) 584–593, https://doi.org/10.5006/1.3287763.

[5] L. Fedrizzi, F. Deflorian, S. Rossi, P.L. Bonora, Study of Aluminium filiform corrosion by using electrochemical techniques, in: Electrochemical Methods in Corrosion Research VI, Trans Tech Publications Ltd, 1998, pp. 485–498, https://doi.org/10.4028/www.scientific.net/MSF.289-292.485.

[6] W.H. Slabaugh, W. Dejager, S.E. Hoover, L.L. Hutchinson, Filiform corrosion of aluminum, J. Paint Technol. 44 (1972) 76–83.

[7] A. Afseth, J.H. Nordlien, G.M. Scamans, K. Nisancioglu, Effect of heat treatment on filiform corrosion of aluminium alloy AA3005, Corros. Sci. 43 (2001) 2093–2109, https://doi.org/10.1016/S0010-938X(01)00014-2.

[8] M. Fedel, F. Deflorian, S. Rossi, Correlations between the Volta potential and filiform corrosion on painted aa2024 aluminum alloy, Surf. Interface Anal. 42 (2010) 199–204, https://doi.org/10.1002/sia.3141.

[9] L. Fedrizzi, M. Stenico, F. Deflorian, S. Maschio, P.L. Bonora, Effect of powder painting procedures on the filiform corrosion of aluminium profiles, Prog. Org. Coat. 59 (2007) 230–238, https://doi.org/10.1016/j.porgcoat.2006.02.011.

[10] M. Fedel, S. Zonta, A. Cristoforetti, Study of ZnAl hydroxides-based thin films to enhance the filiform corrosion resistance of acrylic-coated AA5005, J. Electrochem. Soc. (2024), https://doi.org/10.1149/1945-7111/ad2599.

[11] G. Williams, R. Grace, Chloride-induced filiform corrosion of organic-coated magnesium, Electrochim. Acta 56 (2011) 1894–1903, https://doi.org/10.1016/J.ELECTACTA.2010.09.005.

[12] C. Kousis, P. Keil, N. McMurray Hamilton, G. Williams, The kinetics and mechanism of filiform corrosion affecting organic coated mg alloy surfaces, Corros. Sci. 206 (2022) 110477, https://doi.org/10.1016/J.CORSCI.2022.110477.

[13] G. Williams, C. Kousis, N. McMurray, P. Keil, A mechanistic investigation of corrosion-driven organic coating failure on magnesium and its alloys, Npj Materials Degradation 3 (2019) 41.

[14] R.T. Ruggeri, T.R. Beck, An analysis of mass transfer in filiform corrosion, Corrosion 39 (1983) 452–465, https://doi.org/10.5006/1.3581907.

[15] A. Bautista, Filiform corrosion in polymer-coated metals, Prog. Org. Coat. 28 (1996) 49–58, https://doi.org/10.1016/0300-9440(95)00555-2.

[16] H.N. McMurray, G. Williams, 2.14 - under film/coating corrosion, in: B. Cottis, M. Graham, R. Lindsay, S. Lyon, T. Richardson, D. Scantlebury, H. Stott (Eds.), Shreir's Corrosion, Elsevier, Oxford, 2010, pp. 988–1004, https://doi.org/10.1016/B978-044452787-5.00040-8.

[17] G. Williams, H.N. McMurray, The mechanism of group (I) chloride initiated filiform corrosion on iron, Electrochem. Commun. 5 (2003) 871–877, https://doi.org/10.1016/J.ELECOM.2003.08.008.

[18] A. Cristoforetti, F. Deflorian, S. Rossi, M. Fedel, On the occurrence of filiform corrosion on organic coated carbon steel exposed to cyclic aging test, Corrosion 79 (2023) 1339–1344, https://doi.org/10.5006/4443.

[19] P.P. Leblanc, G.S. Frankel, Investigation of filiform corrosion of epoxy-coated 1045 carbon steel by scanning kelvin probe force microscopy, J. Electrochem. Soc. 151 (2004) B105–B113, https://doi.org/10.1149/1.1641038.

[20] N. Wint, D. Eaves, E. Michailidou, A. Bennett, J.R. Searle, G. Williams, H. N. McMurray, The kinetics and mechanism of filiform corrosion occurring on zinc-aluminium-magnesium coated steel, Corros. Sci. 158 (2019) 108073, https://doi.org/10.1016/j.corsci.2019.06.028.

[21] J.H.W. de Wit, New knowledge on localized corrosion obtained from local measuring techniques, Electrochim. Acta 46 (2001) 3641–3650, https://doi.org/10.1016/S0013-4686(01)00642-9.

[22] W. Schmidt, M. Stratmann, Scanning Kelvinprobe investigations of filiform corrosion on aluminium alloy 2024-T3, Corros. Sci. 40 (1998) 1441–1443, https://doi.org/10.1016/S0010-938X(98)00044-4.

[23] M.G. Olivier, M. Poelman, M. Demuynck, J.P. Petitjean, EIS evaluation of the filiform corrosion of aluminium coated by a cataphoretic paint, Prog. Org. Coat. 52 (2005) 263–270, https://doi.org/10.1016/J.PORGCOAT.2004.05.008.

[24] A. Cristoforetti, J. Izquierdo, R.M. Souto, F. Deflorian, M. Fedel, S. Rossi, In-situ measurement of electrochemical activity related to filiform corrosion in organic coated steel by scanning vibrating electrode technique and scanning micropotentiometry, Corros. Sci. 227 (2024) 111669, https://doi.org/10.1016/j.corsci.2023.111669.

[25] D.A. Worsley, H.N. McMurray, A. Belghazi, Determination of localised corrosion mechanisms using a scanning vibrating reference electrode technique, Chem. Commun. (1997) 2369–2370.

[26] A. Cristoforetti, S. Rossi, F. Deflorian, M. Fedel, An electrochemical study on the mechanism of filiform corrosion on acrylic-coated carbon steel, Prog. Org. Coat. 179 (2023) 107525, https://doi.org/10.1016/j.porgcoat.2023.107525.

[27] T.M. Watson, A.J. Coleman, G. Williams, H.N. McMurray, The effect of oxygen partial pressure on the filiform corrosion of organic coated iron, Corros. Sci. 89 (2014) 46–58, https://doi.org/10.1016/j.corsci.2014.08.004.

[28] S.M. Cambier, D. Verreault, G.S. Frankel, Raman investigation of anodic undermining of coated steel during environmental exposure, Corrosion 70 (2014) 1219–1229, https://doi.org/10.5006/1358.

[29] H. Leidheiser, Corrosion of painted metals—a review, Corrosion 38 (1982) 374–383, https://doi.org/10.5006/1.3581899.

[30] F. Brau, F. Haudin, S. Thouvenel-Romans, A. De Wit, O. Steinbock, S.S.S. Cardoso, J.H.E. Cartwright, Filament dynamics in confined chemical gardens and in filiform corrosion, Phys. Chem. Chem. Phys. 20 (2018) 784–793, https://doi.org/10.1039/c7cp06003c.

[31] N. Wint, D. Eaves, G. Williams, H.N. McMurray, The use of anion exchange pigments to inhibit the filiform corrosion of zinc-aluminium-magnesium coated steel, Corros. Sci. 193 (2021) 109886, https://doi.org/10.1016/J.CORSCI.2021.109886.

[32] G. Williams, Critical factors in the inhibition of filiform corrosion by in-coating ion-exchange pigments, ECS Trans. 24 (2010) 67–76, https://doi.org/10.1149/1.3453607.

[33] M. Van Loo, D.D. Laiderman, R.R. Bruhn, Filiform corrosion, Corrosion 9 (1953) 277–283, https://doi.org/10.5006/0010-9312-9.8.277.

[34] W.H. Slabaugh, M. Grotheer, Mechanism of filiform corrosion, Ind. Eng. Chem. 46 (1954) 1014–1016, https://doi.org/10.1021/ie50533a053.

[35] R.S.T.J. Preston, B. Sanyal, Atmospheric corrosion by nuclei, J. Appl. Chem. 6 (1956) 26–44, https://doi.org/10.1002/jctb.5010060104.

[36] R. Catubig, M. Seter, W. Neil, M. Forsyth, B. Hinton, Effects of corrosion inhibiting pigment lanthanum 4-Hydroxy Cinnamate on the filiform corrosion of coated steel, J. Electrochem. Soc. 158 (2011) C353–C358, https://doi.org/10.1149/2.012111jes.

[37] C.F. Glover, G. Williams, Inhibition of corrosion-driven organic coating delamination and filiform corrosion on iron by phenyl phosphonic acid, Prog. Org. Coat. 102 (2017) 44–52, https://doi.org/10.1016/J.PORGCOAT.2016.03.006.

[38] E.L. Koehler, Influence of contaminants on the failure of protective organic coatings on steel, Corrosion 33 (1977) 209–217, https://doi.org/10.5006/0010-9312-33.6.209.

[39] M.L. Tayler, M. Blanton, C. Konecki, J. Rawlins, J.R. Scully, Scribe creep and Underpaint corrosion on ultra-high molecular weight epoxy resin-coated 1018 steel part 1: comparison of field exposures to standard laboratory accelerated life tests, Corrosion 71 (2014) 71–91, https://doi.org/10.5006/1348.

[40] M.L. Tayler, M. Blanton, C. Konecki, J. Rawlins, J.R. Scully, Scribe creep and Underpaint corrosion on ultra-high molecular weight epoxy resin coated 1018 steel part 2: scribe creep model as a function of environmental severity factors, Corrosion 71 (2014) 326–342, https://doi.org/10.5006/1349.

[41] A. Cristoforetti, S. Rossi, F. Deflorian, M. Fedel, Comparative study between natural and artificial weathering of acrylic-coated steel, aluminum, and galvanized steel, Mater. Corros. 74 (2023) 1429–1438, https://doi.org/10.1002/maco.202313858.

[42] ASTM G85-19, Standard practice for modified salt spray (fog), Testing (2019), https://doi.org/10.1520/G0085-19.

[43] P. Kalenda, M. Petrášek, Study of the resistances of organic coatings to filiform corrosion, Macromol. Symp. 187 (2002) 387–396, https://doi.org/10.1002/1521-3900(200209)187:1<387::AID-MASY387>3.0.CO;2-Q.

[44] M. Morcillo, Soluble salts: their effect on premature degradation of anticorrosive paints, Prog. Org. Coat. 36 (1999) 137–147, https://doi.org/10.1016/S0300-9440(99)00036-3.

[45] R.M. Souto, L. Fernández-Mérida, SECM imaging of interfacial processes in defective organic coatings applied on metallic substrates using oxygen as redox mediator, Electroanalysis 21 (2009) 2640–2646, https://doi.org/10.1002/elan.200900232.
[46] R.M. Souto, Y. González-García, S. González, In situ monitoring of electroactive species by using the scanning electrochemical microscope. Application to the investigation of degradation processes at defective coated metals, Corros. Sci. 47 (2005) 3312–3323, https://doi.org/10.1016/j.corsci.2005.07.005.
[47] A. Alizadeh Razin, B. Ramezanzadeh, H. Yari, Detecting and estimating the extent of automotive coating delamination and damage indexes after stone chipping using electrochemical impedance spectroscopy, Prog. Org. Coat. 92 (2016) 95–109, https://doi.org/10.1016/J.PORGCOAT.2015.11.023.
[48] A. Cristoforetti, F. Deflorian, S. Rossi, M. Fedel, On the limits of the EIS low-frequency impedance Modulus as a tool to describe the protection properties of organic coatings exposed to accelerated aging tests, Coatings 13 (2023) 598, https://doi.org/10.3390/coatings13030598.
[49] ASTM, Standard Test Method for Evaluating Degree of Rusting on Painted Steel Surfaces, ASTM Standards D 610–01, 2001, pp. 1–6, https://doi.org/10.1520/D0610-08R19.2.
[50] ASTM, D2803–09, Standard Guide for Testing Filiform Corrosion Resistance of Organic Coatings on Metal, 2020, https://doi.org/10.1520/D2803-09R20.
[51] A. Miszczyk, K. Darowicki, Effect of environmental temperature variations on protective properties of organic coatings, Prog. Org. Coat. 46 (2003) 49–54.
[52] H. Ochs, J. Vogelsang, Effect of temperature cycles on impedance spectra of barrier coatings under immersion conditions, Electrochim. Acta 49 (2004) 2973–2980, https://doi.org/10.1016/j.electacta.2004.01.056.
[53] C. Vosgien Lacombre, G. Bouvet, D. Trinh, S. Mallarino, S. Touzain, Effect of pigment and temperature onto swelling and water uptake during organic coating ageing, Prog. Org. Coat. 124 (2018) 249–255, https://doi.org/10.1016/j.porgcoat.2017.11.022.
[54] M. Yu, C. Fan, F. Ge, Q. Lu, X. Wang, Z. Cui, Anticorrosion behavior of organic offshore coating systems in UV, salt spray and low temperature alternation simulated Arctic offshore environment, Materials Today Communications 28 (2021) 102545, https://doi.org/10.1016/j.mtcomm.2021.102545.
[55] M. Dornbusch, S. Kirsch, C. Henzel, C. Deschamps, S. Overmeyer, K. Cox, M. Wiedow, U. Tromsdorf, M. Dargatz, U. Meisenburg, Characterization of the water uptake and electrolyte uptake of organic coatings and the consequences by means of electrochemical impedance spectroscopy and UV–vis spectroscopy, Prog. Org. Coat. 89 (2015) 332–343, https://doi.org/10.1016/J.PORGCOAT.2015.03.016.
[56] L.A. Felton, Characterization of coating systems, AAPS PharmSciTech 8 (2007) 112, https://doi.org/10.1208/pt0804112.
[57] G. Hoch, in: R.W. Staehle, B.F. Brown, J. Kruger, A. Agrawal (Eds.), A Review of Filiform Corrosion, Localized Corrosion, NACE-3, 1974. Houston, TX.
[58] W. Funke, Blistering of paint films and filiform corrosion, Prog. Org. Coat. 9 (1981) 29–46, https://doi.org/10.1016/0033-0655(81)80014-3.
[59] W. Funke, Toward a unified view of the mechanism responsible for Paint, Ind. Eng. Chem. Prod. Res. Dev. 24 (1985) 343–347.
[60] G. Williams, H.N. McMurray, D. Hayman, P.C. Morgan, Time-lapse potentiometric imaging of active filiform corrosion using a scanning kelvin probe technique, PhysChemComm 4 (2001) 1–6, https://doi.org/10.1039/b100835h.
[61] J.V. Kloet, W. Schmidt, A.W. Hassel, M. Stratmann, The role of chromate in filiform corrosion inhibition, Electrochim. Acta 48 (2003) 1211–1222, https://doi.org/10.1016/S0013-4686(02)00829-0.
[62] G. Grundmeier, W. Schmidt, M. Stratmann, Corrosion protection by organic coatings: electrochemical mechanism and novel methods of investigation, Electrochim. Acta 45 (2000) 2515–2533, https://doi.org/10.1016/S0013-4686(00)00348-0.
[63] C. Senöz, S. Borodin, M. Stratmann, M. Rohwerder, In situ detection of differences in the electrochemical activity of Al2Cu IMPs and investigation of their effect on FFC by scanning kelvin probe force microscopy, Corros. Sci. 58 (2012) 307–314.
[64] J.D.B. Sharman, J.M. Sykes, T. Handyside, Cathodic disbonding of chlorinated rubber coatings from steel, Corros. Sci. 35 (1993) 1375–1383.
[65] J.D. Bernal, D.R. Dasgupta, A.L. Mackay, The oxides and hydroxides of iron and their structural inter-relationships, Clay Miner. Bull. 4 (1959) 15–30, https://doi.org/10.1180/claymin.1959.004.21.02.
[66] F.T. Rolard, G. Bourrié, M.A. Bdelmoula, P. Refait, F. Dé, R. Feder, Fougerite, A New Mineral of the Pyroaurite-Iowaite Group: Description and Crystal Structure, (n.d.). doi:https://doi.org/10.1346/CCMN.2007.0550308.
[67] A.A. Olowe, J.M.R. Génin, The mechanism of oxidation of ferrous hydroxide in sulphated aqueous media: importance of the initial ratio of the reactants, Corros. Sci. 32 (1991) 965–984, https://doi.org/10.1016/0010-938X(91)90016-I.
[68] R. Aissa, M. Francois, C. Ruby, F. Fauth, G. Medjahdi, M. Abdelmoula, J.-M. Génin, Formation and crystallographical structure of hydroxysulphate and hydroxycarbonate green rusts synthetised by coprecipitation, J. Phys. Chem. Solids 67 (2006) 1016–1019, https://doi.org/10.1016/j.jpcs.2006.01.020.
[69] Ph. Refait, D.D. Nguyen, M. Jeannin, S. Sable, M. Langumier, R. Sabot, Electrochemical formation of green rusts in deaerated seawater-like solutions, Electrochim. Acta 56 (2011) 6481–6488, https://doi.org/10.1016/j.electacta.2011.04.123.
[70] S. Pineau, R. Sabot, L. Quillet, M. Jeannin, Ch. Caplat, I. Dupont-Morral, Ph. Refait, Formation of the Fe (II–III) hydroxysulphate green rust during marine corrosion of steel associated to molecular detection of dissimilatory sulphite-reductase, Corros. Sci. 50 (2008) 1099–1111, https://doi.org/10.1016/j.corsci.2007.11.029.
[71] J.M.R. Génin, P.H. Refait, M. Abdelmoula, Green rusts and their relationship to iron corrosion; a key role in microbially influenced corrosion, Hyperfine Interact. 139–140 (2002) 119–131, https://doi.org/10.1023/A:1021219021919.
[72] C. Rémazeilles, Ph. Refait, On the formation of β-FeOOH (akaganéite) in chloride-containing environments, Corros. Sci. 49 (2007) 844–857, https://doi.org/10.1016/j.corsci.2006.06.003.
[73] D. Neff, P. Dillmann, L. Bellot-Gurlet, G. Beranger, Corrosion of iron archaeological artefacts in soil: characterisation of the corrosion system, Corros. Sci. 47 (2005) 515–535, https://doi.org/10.1016/j.corsci.2004.05.029.
[74] E. Burger, L. Legrand, D. Neff, H. Faiz, S. Perrin, V. L'Hostis, P. Dillmann, In situ structural characterisation of nonstable phases involved in atmospheric corrosion of ferrous heritage artefacts, Corros. Eng. Sci. Technol. 45 (2010) 395–399, https://doi.org/10.1179/147842210X12710800383729.
[75] C. Senöz, M. Rohwerder, Scanning kelvin probe force microscopy for the in situ observation of the direct interaction between active head and intermetallic particles in filiform corrosion on aluminium alloy, Electrochim. Acta 56 (2011) 9588–9595, https://doi.org/10.1016/j.electacta.2011.02.052.
[76] S.B. Lyon, R. Bingham, D.J. Mills, Advances in corrosion protection by organic coatings: what we know and what we would like to know, Prog. Org. Coat. 102 (2017) 2–7, https://doi.org/10.1016/j.porgcoat.2016.04.030.
[77] W. Funke, The role of adhesion in corrosion protection by organic coatings, Journal of the Oil and Colour Chemists' Association 68 (1985) 229–232.
[78] M. Kendig, D.J. Mills, An historical perspective on the corrosion protection by paints, Prog. Org. Coat. 102 (2017) 53–59.
[79] M.K. Harun, J. Marsh, S.B. Lyon, The effect of surface modification on the cathodic disbondment rate of epoxy and alkyd coatings, Prog. Org. Coat. 54 (2005) 317–321, https://doi.org/10.1016/j.porgcoat.2005.07.007.
[80] M.H. Shahini, H. Eivaz Mohammadloo, B. Ramezanzadeh, Recent advances in steel surface treatment via novel/green conversion coatings for anti-corrosion applications: a review study, J. Coat. Technol. Res. 19 (2022) 159–199, https://doi.org/10.1007/s11998-021-00466-0.
[81] J. Marsh, J. Scantlebury, S. Lyon, The effect of surface/primer treatments on the performance of alkyd coated steel, Corros. Sci. 43 (2001) 829–852.
[82] S. Sheikholeslami, G. Williams, H.N. McMurray, L. Gommans, S. Morrison, S. Ngo, D.E. Williams, W. Gao, Cut-edge corrosion behavior assessment of newly developed environmental-friendly coating systems using the scanning vibrating electrode technique (SVET), Corros. Sci. 192 (2021) 109813, https://doi.org/10.1016/j.corsci.2021.109813.
[83] R. Yıldız, I. Dehri, Investigation of the cut-edge corrosion of organically-coated galvanized steel after accelerated atmospheric corrosion test, Arab. J. Chem. 8 (2015) 821–827.
[84] J.B. Jorcin, E. Aragon, C. Merlatti, N. Pébère, Delaminated areas beneath organic coating: a local electrochemical impedance approach, Corros. Sci. 48 (2006) 1779–1790, https://doi.org/10.1016/J.CORSCI.2005.05.031.
[85] E. Brooman, Modifying organic coatings to provide corrosion resistance: part II—inorganic additives and inhibitors, Met. Finish. 100 (2002) 42–53.
[86] A. Kadhim, A. Al-Amiery, R. Alazawi, M. Al-Ghezi, R. Abass, Corrosion inhibitors. A review, International Journal of Corrosion and Scale Inhibition 10 (2021) 54–67.
[87] P.B. Raja, M. Ismail, S. Ghoreishiamiri, J. Mirza, M.C. Ismail, S. Kakooei, A. A. Rahim, Reviews on corrosion inhibitors: a short view, Chem. Eng. Commun. 203 (2016) 1145–1156.
[88] S. Akbarzadeh, M. Ramezanzadeh, B. Ramezanzadeh, Inspection the corrosion prevention performance and dry/wet interfacial adhesion qualities of the melamine-cured polyester coating applied on the treated mild steel surface with a nanostructured composite cerium-neodymium film, Colloids Surf. A Physicochem. Eng. Asp. 590 (2020) 124472.
[89] Z. Mahidashti, T. Shahrabi, B. Ramezanzadeh, The role of post-treatment of an ecofriendly cerium nanostructure conversion coating by green corrosion inhibitor on the adhesion and corrosion protection properties of the epoxy coating, Prog. Org. Coat. 114 (2018) 19–32.
[90] J.M.C. Mol, B.R.W. Hinton, D.H. Van Der Weijde, J.H.W. De Wit, S. Van Der Zwaag, A filiform corrosion and potentiodynamic polarisation study of some aluminium alloys, J. Mater. Sci. 35 (2000) 1629–1639, https://doi.org/10.1023/A:1004795528090.
[91] L. Fedrizzi, F. Deflorian, S. Rossi, P.L. Bonora, Study of aluminium filiform corrosion by using electrochemical techniques, Mater. Sci. Forum 289–292 (1998) 485–498, https://doi.org/10.4028/www.scientific.net/msf.289-292.485.
[92] C.F. Glover, M.L.C. Lim, J.R. Scully, Increased filiform corrosion resistance utilizing a zirconium-based conversion coating on an Al-Zn-Mg-Cu (AA7075-T6) alloy as well as selected surface treatments, Corrosion 77 (2020) 40–52, https://doi.org/10.5006/3510.
[93] A. Cristoforetti, S. Rossi, F. Deflorian, M. Fedel, Exploring the role of passivating conversion coatings in enhancing the durability of organic-coated steel against filiform corrosion using an electrochemical simulated approach, Prog. Org. Coat. 189 (2024) 108357, https://doi.org/10.1016/j.porgcoat.2024.108357.
[94] M. Fedel, M. Zampiccoli, Insight into the role of cerium (III) addition to a MgAl-LDH coating on AA6082, Appl. Sci. 11 (2021) 8252, https://doi.org/10.3390/app11178252.
[95] M.A. Iqbal, L. Sun, A.T. Barrett, M. Fedel, Layered double hydroxide protective films developed on aluminum and aluminum alloys: synthetic methods and anti-corrosion mechanisms, Coatings 10 (2020) 428, https://doi.org/10.3390/coatings10040428.
[96] J. Tedim, M.L. Zheludkevich, A.C. Bastos, A.N. Salak, A.D. Lisenkov, M.G. S. Ferreira, Influence of preparation conditions of layered double hydroxide

conversion films on corrosion protection, Electrochim. Acta 117 (2014) 164–171, https://doi.org/10.1016/j.electacta.2013.11.111.
[97] G. Zhang, E. Jiang, L. Wu, A. Tang, A. Atrens, F. Pan, Active corrosion protection of phosphate loaded PEO/LDHs composite coatings: SIET study, Journal of Magnesium and Alloys 10 (2022) 1351–1357, https://doi.org/10.1016/j.jma.2021.03.008.
[98] L. Guo, W. Wu, Y. Zhou, F. Zhang, R. Zeng, J. Zeng, Layered double hydroxide coatings on magnesium alloys: a review, J. Mater. Sci. Technol. 34 (2018) 1455–1466, https://doi.org/10.1016/j.jmst.2018.03.003.
[99] J. Zuo, Z. Peng, B. Dong, Y. Wang, In situ growth of corrosion resistant mg-Fe layered double hydroxide film on Q235 steel, J. Colloid Interface Sci. 610 (2022) 202–212, https://doi.org/10.1016/j.jcis.2021.12.018.
[100] S. Qin, Y. Wu, C. Zhang, P. Chen, L. Zeng, B. Dong, S. Hong, Acid activation–based growth behaviors and enhanced corrosion resistance of layer-by-layer mg/Al-CO32– layered double hydroxide film on a steel substrate, Appl. Clay Sci. 226 (2022) 106589, https://doi.org/10.1016/j.clay.2022.106589.
[101] S. Hong, S. Qin, Z. Liu, M. Liu, Y. Zhang, B. Dong, Enhanced corrosion resistance and applicability of Mg/Al-CO32– layered double hydroxide film on Q235 steel substrate, Constr. Build. Mater. 276 (2021) 122259, https://doi.org/10.1016/j.conbuildmat.2021.122259.
[102] G.T. Hefter, N.A. North, S.H. Tan, Organic corrosion inhibitors in neutral solutions; part 1 — inhibition of steel, copper, and aluminum by straight chain carboxylates, Corrosion 53 (1997) 657–667, https://doi.org/10.5006/1.3290298.
[103] T.A. Söylev, M.G. Richardson, Corrosion inhibitors for steel in concrete: state-of-the-art report, Constr. Build. Mater. 22 (2008) 609–622, https://doi.org/10.1016/j.conbuildmat.2006.10.013.
[104] K. Tamalmani, H. Husin, Review on corrosion inhibitors for oil and gas corrosion issues, Appl. Sci. 10 (2020) 3389.
[105] Y. Peng, A.E. Hughes, J.I. Mardel, G.B. Deacon, P.C. Junk, R.A. Catubig, M. Forsyth, B.R.W. Hinton, A.E. Somers, Dual function of rare earth carboxylate compounds on the barrier properties and active corrosion inhibition of epoxy coatings on mild steel, Prog. Org. Coat. 185 (2023) 107870, https://doi.org/10.1016/j.porgcoat.2023.107870.
[106] M. Forsyth, K. Wilson, T. Behrsing, C. Forsyth, G.B. Deacon, A. Phanasgoankar, Effectiveness of rare-earth metal compounds as corrosion inhibitors for steel, Corrosion 58 (2002) 953–960.
[107] L. Exbrayat, B. Rameau, M. Uebel, M. Rohwerder, K. Landfester, D. Crespy, E. Campazzi, S. Touzain, J. Creus, New approach using fluorescent nanosensors for filiform corrosion inhibition, Mater. Lett. 318 (2022) 132240, https://doi.org/10.1016/j.matlet.2022.132240.
[108] D. Minudri, A. Somers, N. Casado, M. Forsyth, D. Mecerreyes, Poly(ionic liquid)s having coumarate counter-anions as corrosion inhibitors in acrylic UV coatings, RSC Appl. Polym. 1 (2023) 55–63, https://doi.org/10.1039/D3LP00017F.
[109] E. Michailidou, H.N. Mcmurray, G. Williams, Inhibition of Filiform Corrosion on Organic-Coated Magnesium-Containing Galvanized Steel by Smart-Release Ion Exchange Pigments, (n.d.). doi:https://doi.org/10.1149/08010.0585ecst.
[110] D.T. Nguyen, H.T.X. To, J. Gervasi, Y. Paint, M. Gonon, M.G. Olivier, Corrosion inhibition of carbon steel by hydrotalcites modified with different organic carboxylic acids for organic coatings, Prog. Org. Coat. 124 (2018) 256–266, https://doi.org/10.1016/j.porgcoat.2017.12.006.
[111] A. Cristoforetti, F. Parola, F. Parrino, J. Izquierdo, R.M. Souto, S. Rossi, F. Deflorian, M. Fedel, Sebacate intercalated CaAl layered double hydroxide pigments for corrosion protection of low carbon steel: anion exchange and electrochemical properties, Appl. Clay Sci. 250 (2024) 107300, https://doi.org/10.1016/j.clay.2024.107300.
[112] Y. Cao, D. Zheng, F. Zhang, J. Pan, C. Lin, Layered double hydroxide (LDH) for multi-functionalized corrosion protection of metals: a review, J. Mater. Sci. Technol. 102 (2022) 232–263, https://doi.org/10.1016/J.JMST.2021.05.078.
[113] A.C. Bouali, M. Serdechnova, C. Blawert, J. Tedim, M.G.S. Ferreira, M. L. Zheludkevich, Layered double hydroxides (LDHs) as functional materials for the corrosion protection of aluminum alloys: a review, Appl. Mater. Today 21 (2020) 100857, https://doi.org/10.1016/j.apmt.2020.100857.
[114] G. Williams, H.N. McMurray, Inhibition of filiform corrosion on organic-coated AA2024-T3 by smart-release cation and anion-exchange pigments, Electrochim. Acta 69 (2012) 287–294, https://doi.org/10.1016/j.electacta.2012.03.002.
[115] M.L. Zheludkevich, J. Tedim, M.G.S. Ferreira, “Smart” coatings for active corrosion protection based on multi-functional micro and nanocontainers, Electrochim. Acta 82 (2012) 314–323, https://doi.org/10.1016/J.ELECTACTA.2012.04.095.
[116] S.K. Poznyak, J. Tedim, L.M. Rodrigues, A.N. Salak, M.L. Zheludkevich, L.F. P. Dick, M.G.S. Ferreira, Novel inorganic host layered double hydroxides intercalated with guest organic inhibitors for anticorrosion applications, ACS Appl. Mater. Interfaces 1 (2009) 2353–2362, https://doi.org/10.1021/am900495r.
[117] T. Stimpfling, F. Leroux, H. Hintze-Bruening, Organo-modified layered double hydroxide in coating formulation to protect AA2024 from corrosion, Colloids Surf. A Physicochem. Eng. Asp. 458 (2014) 147–154, https://doi.org/10.1016/j.colsurfa.2014.01.042.
[118] S.P.V. Mahajanam, R.G. Buchheit, Characterization of inhibitor release from Zn-Al-$[V10O28]^{6-}$ Hydrotalcite pigments and corrosion protection from Hydrotalcite-pigmented epoxy coatings, Corrosion 64 (2008) 230–240, https://doi.org/10.5006/1.3278468.
[119] M.L. Zheludkevich, S.K. Poznyak, L.M. Rodrigues, D. Raps, T. Hack, L.F. Dick, T. Nunes, M.G.S. Ferreira, Active protection coatings with layered double hydroxide nanocontainers of corrosion inhibitor, Corros. Sci. 52 (2010) 602–611, https://doi.org/10.1016/j.corsci.2009.10.020.
[120] D. Li, F. Wang, X. Yu, J. Wang, Q. Liu, P. Yang, Y. He, Y. Wang, M. Zhang, Anticorrosion organic coating with layered double hydroxide loaded with corrosion inhibitor of tungstate, Prog. Org. Coat. 71 (2011) 302–309, https://doi.org/10.1016/j.porgcoat.2011.03.023.
[121] D. Grigoriev, Chapter 8- intelligent coatings for corrosion control, in: Anticorrosion Coatings with Self-Recovering Ability Based on Damage-Triggered Micro- and Nanocontainers, Elsevier Inc., 2015, pp. 283–333, https://doi.org/10.1016/B978-0-12-411467-8.00008-8.
[122] S.P. Newman, W. Jones, Synthesis, characterization and applications of layered double hydroxides containing organic guests, New J. Chem. 22 (1998) 105–115, https://doi.org/10.1039/a708319j.
[123] F. Millange, R.I. Walton, L. Lei, D. O'Hare, Efficient separation of terephthalate and phthalate anions by selective ion-exchange intercalation in the layered double hydroxide $Ca_2Al(OH)_6{\cdot}NO_3{\cdot}2H_2O$, Chem. Mater. 12 (2000) 1990–1994, https://doi.org/10.1021/CM0002057.
[124] S. Miyata, Anion-exchange properties of hydrotalcite-like compounds, Clay Clay Miner. 31 (1983) 305–311, https://doi.org/10.1346/CCMN.1983.0310409.
[125] M. Meyn, K. Beneke, G. Lagaly, Anion-exchange reactions of layered double hydroxides, Inorg. Chem. 29 (1990) 5201–5207, https://doi.org/10.1021/ic00351a013.
[126] T. Kameda, Y. Miyano, T. Yoshioka, M. Uchida, A. Okuwaki, New treatment methods for waste water containing chloride ion using magnesium-aluminum oxide, Chem. Lett. (2000) 1136–1137, https://doi.org/10.1246/cl.2000.1136.
[127] Y. Chen, Z. Shui, W. Chen, G. Chen, Chloride binding of synthetic Ca–Al–NO_3 LDHs in hardened cement paste, Constr. Build. Mater. 93 (2015) 1051–1058, https://doi.org/10.1016/j.conbuildmat.2015.05.047.
[128] G. Williams, H.N. McMurray, Anion-exchange inhibition of filiform corrosion on organic coated AA2024-T3 aluminum alloy by Hydrotalcite-like pigments, Electrochem. Solid-State Lett. 6 (2003) B9, https://doi.org/10.1149/1.1539771.
[129] J. Sullivan, N. Cooze, C. Gallagher, T. Lewis, T. Prosek, D. Thierry, In situ monitoring of corrosion mechanisms and phosphate inhibitor surface deposition during corrosion of zinc–magnesium–aluminium (ZMA) alloys using novel time-lapse microscopy, Faraday Discuss. 180 (2015) 361–379, https://doi.org/10.1039/C4FD00251B.
[130] R. Hausbrand, M. Stratmann, M. Rohwerder, Corrosion of zinc–magnesium coatings: mechanism of paint delamination, Corros. Sci. 51 (2009) 2107–2114, https://doi.org/10.1016/j.corsci.2009.05.042.
[131] R. Hausbrand, M. Stratmann, M. Rohwerder, Delamination resistant zinc alloys: simple concept and results on the system zinc-magnesium, Steel Res. Int. 74 (2003) 453–458, https://doi.org/10.1002/srin.200300212.
[132] N. Wint, D. Eaves, G. Williams, H.N. McMurray, The effect of composition and thickness on the mechanism and kinetics of filiform corrosion occurring on zinc-aluminium-magnesium coated steel, Corros. Sci. 179 (2021) 109168, https://doi.org/10.1016/J.CORSCI.2020.109168.
[133] T. Suzuki, H. Ikeda, Studi of filiform corrosion of coated aluminum, Sumimoto Light Metal Technical Reports 20 (1979) 12–22.
[134] S.S. Jamali, D.J. Mills, Steel surface preparation prior to painting and its impact on protective performance of organic coating, Prog. Org. Coat. 77 (2014) 2091–2099, https://doi.org/10.1016/j.porgcoat.2014.08.001.
[135] P. Pedeferri, Corrosion Science and Engineering, 1st ed., Springer Cham, Springer Nature Switzerland, 2018.